Article

Cooperative Metal–Boron Interactions in the Reaction of *nido*-1,2-(Cp*RuH)BH, Cp* = η⁵-CMe, with HC#CPh

Hong Yan, Bruce C. Noll, and Thomas P. Fehlner

J. Am. Chem. Soc., **2005**, 127 (13), 4831-4844• DOI: 10.1021/ja042439n • Publication Date (Web): 11 March 2005

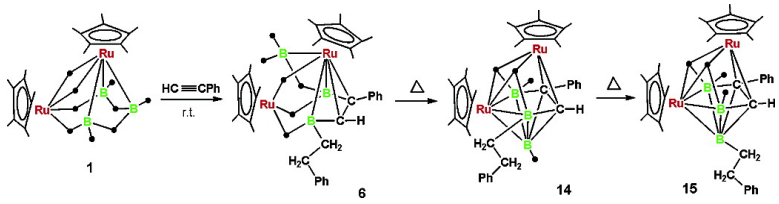

More About This Article

Additional resources and features associated with this article are available within the HTML version:

- Supporting Information
- Links to the 3 articles that cite this article, as of the time of this article download
- Access to high resolution figures
- Links to articles and content related to this article
- Copyright permission to reproduce figures and/or text from this article

View the Full Text HTML

J|A|C|S
ARTICLES
Published on Web 03/11/2005

Cooperative Metal−Boron Interactions in the Reaction of *nido*-1,2-$(Cp^*RuH)_2B_3H_7$, $Cp^* = \eta^5$-C_5Me_5, with HC≡CPh

Hong Yan,*,† Bruce C. Noll, and Thomas P. Fehlner*

Contribution from the Department of Chemistry and Biochemistry, University of Notre Dame, Notre Dame, Indiana 46556-5670

Received December 16, 2004; E-mail: Hong.Yan.13@nd.edu; fehlner.1@nd.edu

Abstract: Products of the reaction of *nido*-1,2-$(Cp^*RuH)_2B_3H_7$, **1**, and phenylacetylene demonstrate the ways in which cluster metal and main group fragments can combine with an alkyne. Observed at 22 °C are (a) reduction to μ-alkylidene Ru−B bridges (isomers *nido*-1,2-$(Cp^*Ru)_2$(1,5-μ-C{Ph}Me)B_3H_7, **2**, and *nido*-1,2-$(Cp^*Ru)_2$(1,5-μ-C{CH_2Ph}H)B_3H_7, **3**), (b) reduction to *exo*-cluster alkyl substituents on boron (*nido*-1,2-$(Cp^*RuH)_2$-3-CH_2CH_2Ph-B_3H_6, **4**), (c) cluster insertion with extrusion of a BH_2 fragment into an *exo*-cluster bridge (*nido*-1,2-$(Cp^*Ru)_2$(μ-H)(μ-BH_2)-4-or-5-Ph-4,5-$C_2B_2H_5$, **5**), (d) combined insertion with BH_2 extrusion and reduction (*nido*-1,2-$(Cp^*Ru)_2$(μ-H)(μ-BH_2)-3-CH_2CH_2Ph-5-Ph-4,5-$C_2B_2H_4$, **6**), (e) insertion and loss of borane with and without reduction (*nido*-1,2-$(Cp^*Ru)_2$-5-Ph-4,5-$C_2B_2H_7$, **7**, and isomers *nido*-1,2-$(Cp^*Ru)_2$-3-CH_2CH_2Ph-4-(and-5-)Ph-$C_2B_2H_6$, **8** and **9**), and (f) insertion and borane loss plus reduction (*nido*-1,2-$(Cp^*Ru)_2$-3-(*trans*-CH═CHPh)-5-Ph-4,5-$C_2B_2H_6$, **10**). Along with **7**, **8**, and **10**, the reaction at 90 °C generates products of insertion and *nido*- to *closo*-cluster closure (*closo*-4-Ph-1,2-$(Cp^*RuH)_2$-4,6-$C_2B_2H_3$, **11**, *closo*-1,2-$(Cp^*RuH)_2$-3-CH_2CH_2Ph-5-Ph-7-CH_2CH_2Ph-4,5-$C_2B_3H_2$, **12**, *closo*-1,2-$(Cp^*RuH)_2$-5-Ph-4,5-$C_2B_3H_4$, **13**, and isomers *closo*-1,2-$(Cp^*RuH)_2$-3-and-7-CH_2CH_2Ph-5-Ph-4,5-$C_2B_3H_3$, **14** and **15**). The clusters with an *exo*-cluster bridging BH_2 groups are shown to be intermediates by demonstrating that the major products **5** and **6** rearrange to **13** and convert to **14**, respectively. **14** then isomerizes to **15**, thus connecting low- and high-temperature products. Finally, all available information shows that the high reactivity of **1** with alkynes can be associated with the "extra" two Ru−H hydrides on the framework of **1** which are required to meet the *nido*-cluster electron count.

Introduction

The development of a general and effective route to metallaboranes from reactions of $[Cp^*MCl_x]_n$, $Cp^* = \eta^5$-C_5Me_5 (groups 5−9), and monoboranes[1,2] makes the systematic reaction chemistry for this class of compounds accessible. Thermal elimination reactions lead to loss of small fragments, e.g., H_2 or BH, to generate more dense and stable structures.[3−6] Addition of metal fragments or monoboranes leads to metal fragment replacement, BH displacement, or cluster expansion.[7−16] Addition of Lewis bases leads to products arising from the competition between metal and boron sites for the base.[17−25] Subsequently, borane displacement vs metal fragment displacement, ligand substitution at metal vs boron sites, and *ortho*-metalation to metal vs boron sites in the case of aromatic bases are observed.[26−28] These reaction types parallel reactions found in transition-metal cluster chemistry and in borane chemistry. In some cases, the reactions reflect a blend of both, consistent with the hybrid character of a metallaborane.[29−35]

† Present address: The State Key Laboratory of Coordination Chemistry, Nanjing University, Nanjing 210093, China.

(1) Fehlner, T. P. *J. Chem. Soc., Dalton Trans.* **1998**, 1525.
(2) Fehlner, T. P. *Organometallics* **2000**, *19*, 2643.
(3) Lei, X.; Shang, M.; Fehlner, T. P. *J. Am. Chem. Soc.* **1999**, *121*, 1275.
(4) Morrey, J. R.; Johnson, A. B.; Fu, Y. C.; Hill, G. R. *Adv. Chem. Ser.* **1961**, *32*, 157.
(5) Venable, T. L.; Grimes, R. N. *Inorg. Chem.* **1982**, *21*, 887.
(6) Bould, J.; Greenwood, N. N.; Kennedy, J. D. *J. Organomet. Chem.* **1983**, *249*, 11.
(7) Hashimoto, H.; Shang, M.; Fehlner, T. P. *J. Am. Chem. Soc.* **1996**, *118*, 8164.
(8) Peldo, M. A.; Beatty, A. M.; Fehlner, T. P. *Organometallics* **2002**, *21*, 2821.
(9) Ghosh, S.; Lei, X. J.; Shang, M. Y.; Fehlner, T. P. *Inorg. Chem.* **2000**, *39*, 5373.
(10) Lei, X. J.; Shang, M. Y.; Fehlner, T. P. *J. Am. Chem. Soc.* **1998**, *120*, 2686.
(11) Lei, X. J.; Shang, M. Y.; Fehlner, T. P. *Chem.—Eur. J.* **2000**, *6*, 2653.
(12) Macías, R.; Holub, J.; Kennedy, J. D.; Stíbr, B.; Thornton-Pett, M. *Chem. Commun*. **1994**, 2265.
(13) Ghosh, S.; Beatty, A. M.; Fehlner, T. P. *Angew. Chem., Int. Ed.* **2003**, *42*, 4678.
(14) Ghosh, S.; Shang, M. Y.; Li, Y. P.; Fehlner, T. P. *Angew. Chem., Int. Ed.* **2001**, *40*, 1125.
(15) Ghosh, S.; Beatty, A. M.; Fehlner, T. P. *J. Am. Chem. Soc.* **2001**, *123*, 9188.
(16) Ghosh, S.; Rheingold, A. L.; Fehlner, T. P. *Chem. Commun.* **2001**, 895.
(17) Kawano, Y.; Matsumoto, H.; Shimoi, M. *Chem. Lett.* **1999**, 489.
(18) Pangan, L. N.; Kawano, Y.; Shimoi, M. *Organometallics* **2000**, *19*, 5575.
(19) Pangan, L. N.; Kawano, Y.; Shimoi, M. *Inorg. Chem.* **2001**, *40*, 1985.
(20) Macías, R.; Fehlner, T. P.; Beatty, A. M. *Angew. Chem., Int. Ed.* **2002**, *41*, 3860.
(21) Macías, R.; Fehlner, T. P.; Beatty, A. M. *Organometallics* **2004**, *23*, 2124.
(22) Housecroft, C. E.; Buhl, M. L.; Long, G. L.; Fehlner, T. P. *J. Am. Chem. Soc.* **1987**, *109*, 3323.
(23) Barton, L.; Bould, J.; Fang, H.; Hupp, K.; Rath, N. P.; Gloeckner, C. *J. Am. Chem. Soc.* **1997**, *119*, 631.
(24) Macias, R.; Rath, N. P.; Barton, L. *Angew. Chem., Int. Ed.* **1999**, *38*, 162.
(25) McQuade, P.; Hupp, K.; Bould, J.; Fang, H.; Rath, N. P.; Thomas, R. L.; Barton, L. *Inorg. Chem.* **1999**, *38*, 5415.
(26) Lei, X. J.; Shang, M. Y.; Fehlner, T. P. *Organometallics*, **2000**, *19*, 5266.
(27) Deaming, A. J.; Kabir, S. E.; Powell, N. I.; Bates, P. A.; Hursthouse, M. B. *J. Chem. Soc., Dalton Trans.* **1987**, 1529.
(28) Crook, J. E.; Greenwood, N. N.; Kennedy, J. D.; McDonald, W. S. *Chem. Commun.* **1982**, 383.
(29) Grimes, R. N. *Acc. Chem. Res*. **1978**, *11*, 420.

Scheme 1. Reaction Products Observed with MeC≡CMe

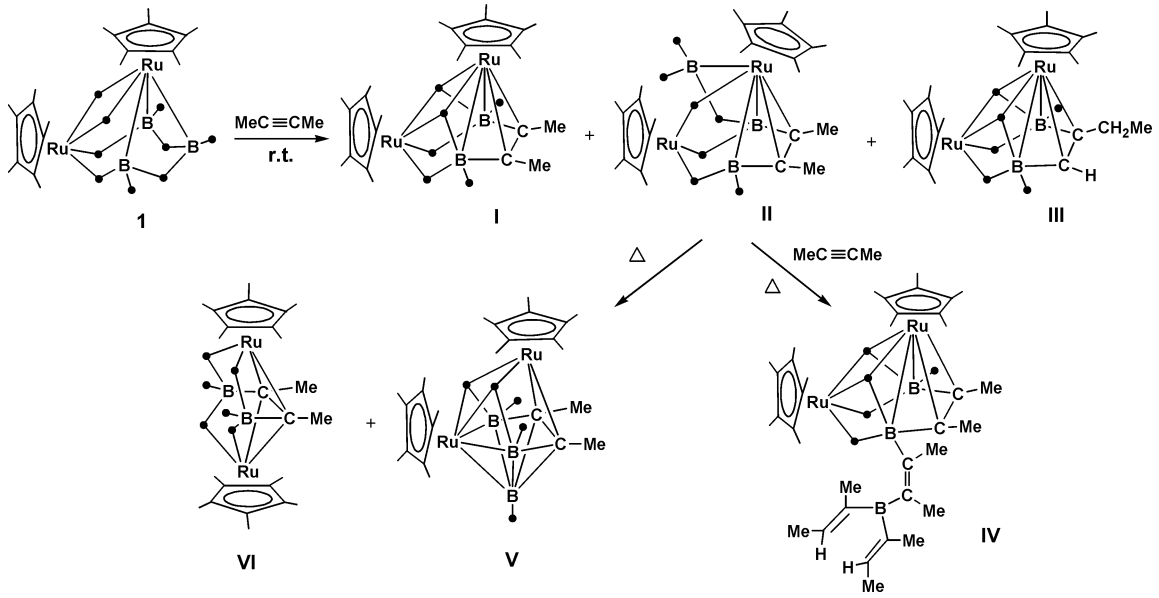

The reactivity of transition-metal complexes and clusters as well as boron hydrides with alkynes is well documented.[36−40] This includes the syntheses of organometallic complexes and catalysis of organic reactions in the case of metal complexes[41,42] and organoboranes, alkenylboranes, and carboranes in the case of boranes.[43−47] So why, then, are there not many examples of the reactions of metallaboranes with alkynes? It is not for lack of trying as back in the 1970s the reaction of an alkyne with a cobaltaborane was shown to generate a cobaltacarborane.[48−50] Little further development occurred possibly due to lack of good synthetic routes to metallaboranes and/or the harsh reaction conditions required.[51−53] But there is more to it than that. Despite the fact that the metallaboranes we have studied, which include metals ranging from group 6 to group 9, readily react with Lewis bases, facile reaction of alkynes with metallaboranes in which the alkyne is incorporated into the cluster structure in some fashion is restricted to ruthenaboranes to date.

Thus, earlier work has shown that the ruthenaborane *nido*-1,2-$(Cp^*RuH)_2B_3H_7$ generates ruthenacarboranes from alkynes.[54−57] For instance, the internal alkyne MeC≡CMe inserts to produce novel metallacarboranes, some of which undergo further conversions (Scheme 1). On the other hand, the activated terminal alkyne HC≡CCO_2Me has significant added reactivity. Metallacarboranes are formed (Scheme 2), but also the first examples of M−B μ-alkylidene complexes result from the cooperative reactivities of the metal hydride and boron hydride fragments of the metallaborane cluster framework. Moreover, the alkyne substituent is involved in an unexpected sequence of chemical transformations, e.g., C═O coordination, C−O bond cleavage, and O insertion into a B−H bond (Scheme 3). Alkyne substituents clearly have a significant effect on reaction chemistry.

Despite these existing studies, an important question remains to be answered. What is the structural feature associated with the ruthenaborane that promotes facile reaction with alkynes? To answer this question, we need additional information, and we have sought it by continuing to address cluster−alkyne reactivity as a function of alkyne substituent. Do the variety of products observed arise from a set of common intermediates with rates of formation controlled by substituent type? Very little information of this type exists for metallaboranes in general, and here, it also contains a key to understanding the thus far unique reactivity of ruthenaboranes. The present study is focused on reaction with HC≡CPh, but the empirical observations provide an answer to the more general question posed.

Results and Discussion

The reaction of *nido*-1,2-$(Cp^*Ru)_2B_3H_9$, **1**, with HC≡CPh was explored at two different temperatures, and the products isolated by chromatography were characterized with spectro-

(30) Grimes, R. N. In *Metal Interactions with Boron Clusters*; Grimes, R. N., Ed.; Plenum: New York, 1982; p 269.
(31) Kennedy, J. D. Prog. *Inorg. Chem*. **1984**, *32*, 519.
(32) Kennedy, J. D. *Prog. Inorg. Chem*. **1986**, *34*, 211.
(33) Housecroft, C. E. *Boranes and Metalloboranes*; Ellis Horwood: Chichester, U.K., 1990.
(34) Smith, M. R., II. *Prog. Inorg. Chem*. **1999**, *48*, 505.
(35) Jan, D. Y.; Workman, D. P.; Hsu, L. Y.; Krause, J. A.; Shore, S. G. *Inorg. Chem*. **1992**, *31*, 5123.
(36) Youngs, W. J.; Tessier, C. A.; Bradshaw, J. D. *Chem. Rev*. **1999**, *99*, 3153.
(37) Szymanska-Buzar, T. *Coord. Chem. Rev*. **1997**, *159*, 205.
(38) Welker, M. E. *Chem. Rev*. **1992**, *92*, 97, 363.
(39) Wojcick, A.; Shuchart, C. E. *Coord. Chem. Rev*. **1990**, *105*, 35.
(40) Bruce, M. I. *Pure Appl. Chem*. **1990**, *62*, 1021.
(41) Coates, G. E.; Green, M. L. H.; Wade, K. *Organometallic Compounds*, 3rd ed.; Methuen: London, 1967.
(42) Elschenbroich, C.; Salzer, A. *Organometallics*; VCH: New York, 1989.
(43) Wilczynski, R.; Snedden, L. G. *J. Am. Chem. Soc*. **1980**, *102*, 2857.
(44) Wilczynski, R.; Snedden, L. G. *Inorg. Chem*. **1981**, *20*, 3955.
(45) Wilczynski, R.; Snedden, L. G. *Inorg. Chem*. **1982**, *21*, 506.
(46) Muetterties, E. L., Ed. *Boron Hydride Chemistry*; Academic Press: New York, 1975.
(47) Grimes, R. N. *Carboranes*; Academic Press: New York, 1970.
(48) Grimes, R. N. *Pure Appl. Chem*. **1974**, *39*, 455.
(49) Weiss, R.; Bowser, J. R.; Grimes, R. N. *Inorg. Chem*. **1978**, *17*, 1522.
(50) Grimes, R. N.; Beer, D. C.; Sneddon, L. G.; Miller, V. R.; Weiss, R. *Inorg. Chem*. **1974**, *13*, 1138.
(51) Ditzel, E. J.; Fontaine, X. L. R.; Greenwood, N. N.; Kennedy, J. D.; Sisan, Z.; Stíbr, B.; Thornton-Pett, M. *Chem. Commun*. **1990**, 1741.
(52) Bould, J.; Rath, N. P.; Barton, L.; Kennedy, J. D. *Organometallics* **1998**, *17*, 902.
(53) Bould, J.; Rath, N. P.; Barton, L. *Organometallics* **1996**, *15*, 4916.
(54) Yan, H.; Beatty, A. M.; Fehlner, T. P. *Angew. Chem., Int. Ed*. **2002**, *41*, 2578.
(55) Yan, H.; Beatty, A. M.; Fehlner, T. P. *J. Organomet. Chem*. **2003**, *680*, 66.
(56) Yan, H.; Beatty, A. M.; Fehlner, T. P. *J. Am. Chem. Soc*. **2002**, *124*, 10280.
(57) Yan, H.; Beatty, A. M.; Fehlner, T. P. *J. Am. Chem. Soc*. **2003**, *125*, 16367.

Scheme 2. Selected Reactivity Observed in the HC≡CC(O)OMe Reaction System

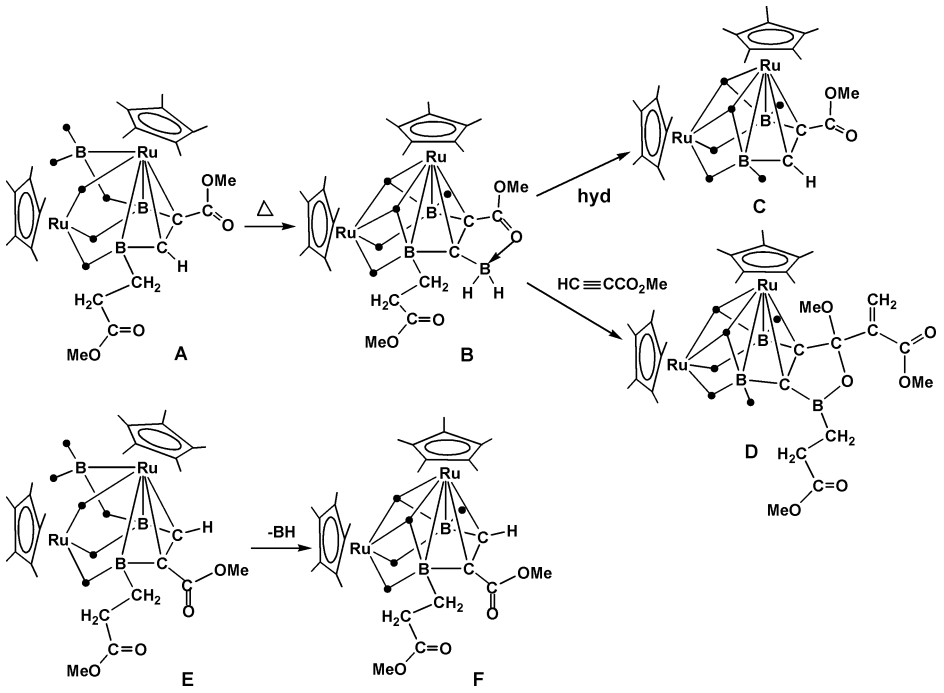

Scheme 3. Some Reaction Products Observed with HC≡CC(O)OMe

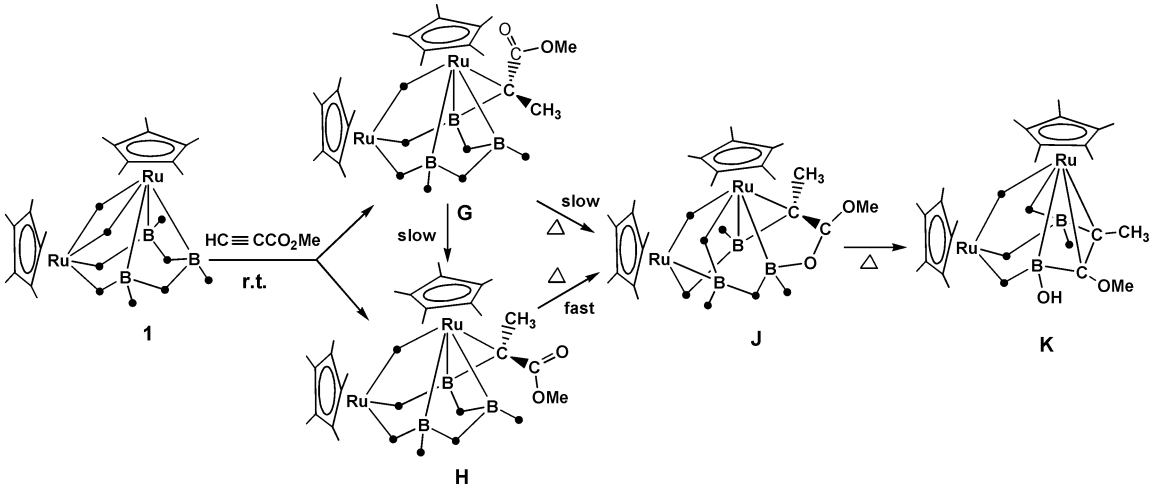

scopic data and X-ray crystal structure determinations. Connections between ambient and higher temperature products were defined by heating isolated ambient temperature products. Some intermediates in the reaction at ambient temperature were characterized in situ by measuring NMR spectra as a function of time.

Ambient Temperature. The reaction of **1** with HC≡CPh at ambient temperature generates a complex reaction mixture from which products **2**−**10** were isolated, accounting for 67% of the ruthenaborane starting material. Two of these products, **6** and **7**, account for 39% or 60% of the total moles of isolated products. Selected spectroscopic data are presented for crystallographically characterized compounds as the spectra/structure correlations are used to define reasonable structures for the intermediates characterized in situ.

***nido*-1,2-(Cp*Ru)$_2$(1,5-μ-C{Ph}Me)B$_3$H$_7$, 2**, was isolated in a yield of 3%. The X-ray structure, shown in Figure 1, displays a Ru−B μ-alkylidene ligand derived from the Markovnikoff addition of two framework hydrogen atoms to

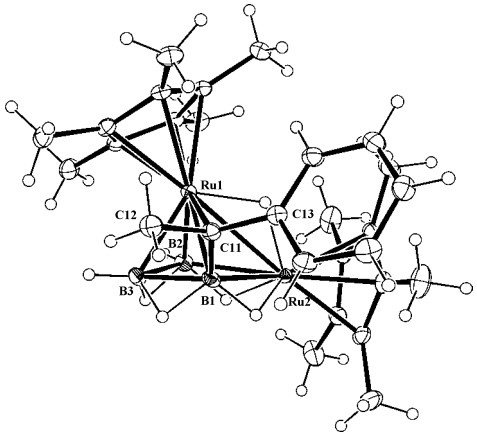

Figure 1. Molecular structure of **2**. Selected bond lengths (Å): B(2)−B(3), 1.826(3); B(2)−Ru(1), 2.165(2); B(2)−Ru(2), 2.317(2); Ru(1)−B(3), 2.125(2); Ru(1)−B(1), 2.131(2); Ru(1)−C(11), 2.2825(18); Ru(1)−Ru(2), 2.8733(2); Ru(2)−B(1), 2.378(2); B(1)−C(11), 1.496(3); B(1)−B(3), 1.839(3); C(11)−C(13), 1.507(3); C(11)−C(12), 1.529(3).

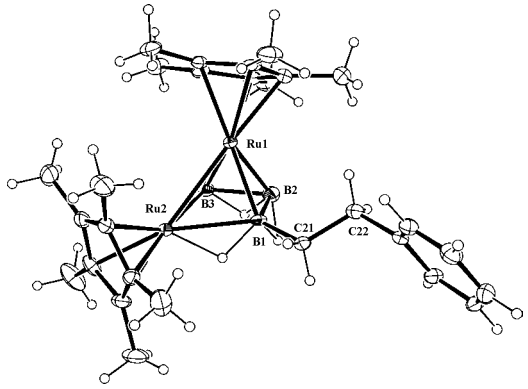

Figure 2. Molecular structure of **4**. Selected bond lengths (Å): Ru(1)−B(2), 2.138(5); Ru(1)−B(1), 2.195(5); Ru(1)−Ru(2), 2.8425(5); Ru(2)−B(3), 2.375(5); B(1)−C(21), 1.615(7); B(1)−B(2), 1.855(8); B(2)−B(3), 1.821(8); C(21)−C(22), 1.550(6); Ru(1)−B(3), 2.173(5); Ru(2)−B(1), 2.437(5).

the alkyne. In **2**, the phenyl group points toward the Ru−Ru edge. ^{1}H NMR data confirm that **2** has one methyl group, one edge-bridging Ru−H−Ru proton, two broad B−H−Ru protons, and two B−Ht protons. Although the other isomer of Markovnikoff addition with the substituent pointing away from the Ru−Ru bond was observed in the reaction with HC≡CCO_2Me,[57] a similar isomer of **2** was not isolated here. The Ru−B μ-alkylidene complex resulting from anti-Markovnikoff addition of the alkyne, **3**, was reported earlier by us[55] and also has the phenyl group pointed toward the Ru−Ru edge. Only terminal alkynes lead to these Ru−B μ-alkylidene complexes; the varieties and yields depend on the alkyne substituent.

***nido*-1,2-(Cp*RuH)$_2$-3-CH_2CH_2Ph-B_3H_6, 4**, was isolated in a yield of 9%. The X-ray determination only defines the framework as five of the framework hydrogen atoms are not found (Figure 2 and Scheme 4). However, the ^{1}H NMR data show their presence in a number consistent with the 7 skeletal electron pair (sep) count required by the *nido* structure. The square pyramidal geometry of **1** is retained, and substitution and hydrometalation take place at the B(3) site. The fully reduced alkyne is produced as a terminal substituent on a boron atom. Thus, the ^{13}C NMR data show broad BCH_2 and sharp CH_2 resonances from a BCH_2CH_2Ph group. The ^{1}H NMR data show resonances corresponding to two CH_2 groups (multiplets), as well as two B−Ht protons, two B−H−Ru protons, two B−H−B protons, one Ru−H−Ru proton (sharp), and one Ru−H(B)−Ru proton (broad). Hence, compared to **1,** one H atom of a B−Ht fragment is replaced by a hydrocarbyl unit generated by full reduction of the alkyne.

Curiously, **4** possesses two more hydrogen atoms than the two reactants combined. Styrene is a byproduct (observed by NMR), but the direct reaction of **1** with H_2C═CHPh did not produce **4** under similar reaction conditions. Further, the μ-alkylidene compound **3** does not covert to **4** when heated with an excess of BH_3·THF. We can only suggest that the "extra" hydrogen atoms for the complete alkyne reduction in **4** are generated from the participation of a second molecule of **1**.

***nido*-1,2-(Cp*Ru)$_2$(μ-H)(μ-BH_2)-4-(or-5)-Ph-4,5-$C_2B_2H_5$, 5**, was isolated in a yield of 5%. Spectroscopic data support the postulated structure shown in Scheme 4. The ^{11}B NMR spectrum reveals three boron resonances in a ratio of 1:1:1. The ^{1}H NMR spectrum shows resonances corresponding to three inequivalent B−Ht protons, one B−H−B proton, two B−H−Ru protons, and one Ru−H−Ru proton and the characteristic broad peak of a B−CH proton confirming alkyne insertion. Both 1D and 2D ^{1}H spectra rule out the presence of a $-CH_2CH_2$Ph group. The precise mass measurement displays a molecular ion peak confirming the composition suggested by NMR. The presence of an *exo*-BH_2 unit is suggested by the NMR data when compared with data on earlier compounds containing this structural feature and characterized by solid-state structures, e.g., **II** in Scheme 1. Corroboration comes from the conversion of **5** to a *closo* 3B species upon heating as related below. Note that the Ph group can occupy either the 4- or 5-position.

***nido*-1,2-(Cp*Ru)$_2$(μ-H)(μ-BH_2)-3-CH_2CH_2Ph-5-Ph-4,5-$C_2B_2H_4$, 6**, was isolated in a yield of 19% and is one of two major products at ambient temperature. Its solid-state structure reveals an *exo*-cluster bridging BH_2 unit, an inserted alkyne, and a terminal hydrocarbyl substituent at the B(3) position (Figure 3). The spectroscopic data are fully consistent with the X-ray structure. Two complex multiplets in the ^{1}H NMR spectrum as well as one sharp and one broad aliphatic carbon resonance in the ^{13}C NMR spectrum are characteristic of a fully reduced alkyne. Moreover, the ^{1}H NMR spectrum displays the

Scheme 4. Reaction Products Observed with HC≡CPh at Ambient Temperature

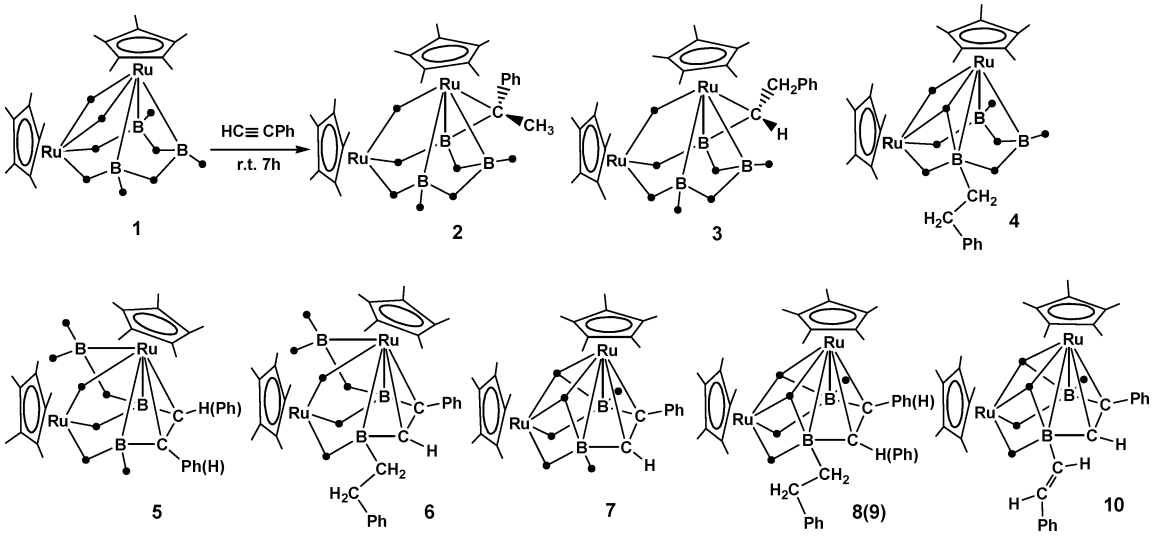

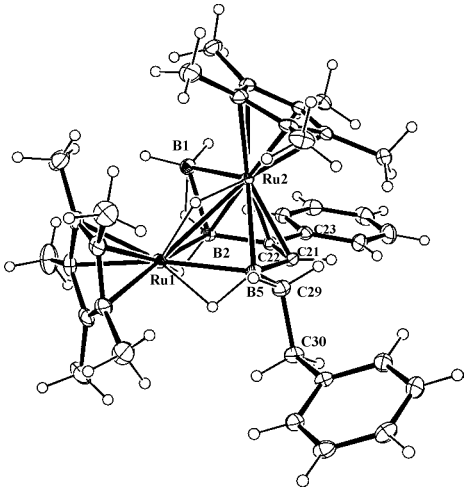

Figure 3. Molecular structure of **6**. Selected bond lengths (Å): Ru(1)−B(5), 2.313(2); Ru(1)−B(2), 2.3197(19); Ru(1)−Ru(2), 2.92940(18); Ru(2)−B(2), 2.1623(19); Ru(2)−C(22), 2.2299(16); Ru(2)−C(21), 2.2307(16); Ru(2)−B(1), 2.287(2); Ru(2)−B(5), 2.4292(19); B(1)−B(2), 1.783(3); B(2)−C(22), 1.551(3); B(5)−C(21), 1.527(3); B(5)−C(29), 1.595(3); C(21)−C(22), 1.421(2); C(22)−C(23), 1.490(2); C(29)−C(30), 1.544(2).

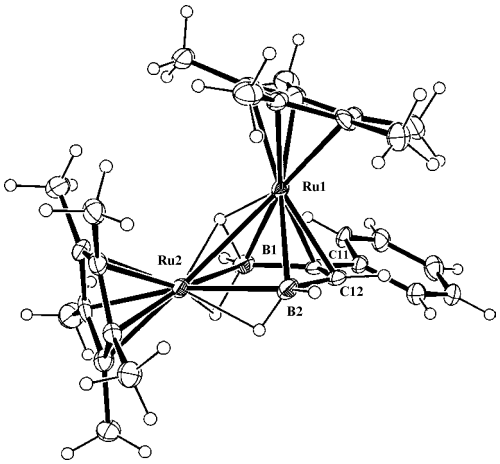

Figure 4. Molecular structure of **7**. Selected bond lengths (Å): Ru(1)−C(12), 2.178(6); Ru(1)−C(11), 2.220(5); Ru(1)−B(1), 2.374(8); Ru(2)−B(2), 2.349(8); B(1)−C(11), 1.585(12); B(2)−C(12), 1.541(10); C(11)−C(12), 1.395(10); Ru(1)−B(2), 2.360(8); Ru(1)−Ru(2), 2.9366(6); Ru(2)−B(1), 2.387(7).

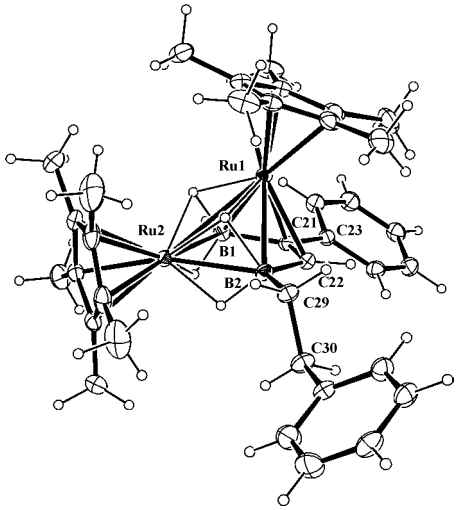

Figure 5. Molecular structure of **8**. Selected bond lengths (Å): Ru(1)−C(21), 2.224(2); Ru(1)−C(22), 2.191(2); Ru(1)−B(1), 2.347(3); Ru(2)−B(1), 2.392(2); Ru(2)−B(2), 2.376(2); B(1)−C(21), 1.561(3); B(2)−C(29), 1.609(4); B(2)−C(22), 1.538(3); C(21)−C(22), 1.420(3); C(21)−C(23), 1.480(3); C(29)−C(30), 1.535(3); Ru(1)−B(2), 2.378(2); Ru(1)−Ru(2), 2.9384(2).

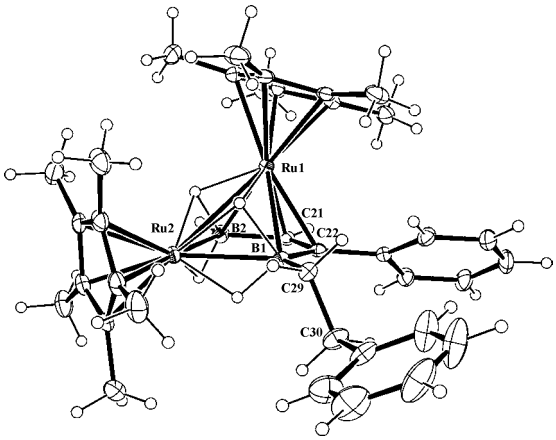

Figure 6. Molecular structure of **9**. Selected bond lengths (Å): Ru(1)−Ru(2), 2.9296(2); Ru(1)−B(1), 2.368(2); Ru(1)−B(2), 2.364(2); Ru(1)−C(21), 2.176(2); Ru(1)−C(22), 2.216(2); Ru(2)−B(2), 2.361(2); Ru(2)−B(1), 2.427(2); B(1)−C(22), 1.565(3); B(2)−C(21), 1.533(3); C(21)−C(22), 1.426(3); B(1)−C(29), 1.605(3); C(29)−C(30), 1.531(3).

two inequivalent B−Ht resonances of the *exo*-cluster BH_2 unit and the one broad resonance of the BC−H fragment of the inserted alkyne.

Compound **6** is the analogue of **A** (Scheme 2); however, the analogue of the isomer corresponding to **E** was not isolated. The presence of an *exo*-cluster BH_2 bridging group places **6** in the same basic cluster category as **II** (Scheme 1) and **5**, both of which lack a terminal hydrocarbyl group. Previous work has demonstrated that species bearing an *exo*-cluster BH_2 fragment are intermediates that undergo interesting transformations.[54,55,57] Hence, **6** is viewed as a kinetic product and, as discussed below, does indeed generate additional products on heating (see below).

***nido*-1,2-(Cp*Ru)$_2$-5-Ph-4,5-$C_2B_2H_7$, 7**, is the other major product. It is air sensitive and was isolated in 20% yield. The solid-state structure shows a *nido*-$Ru_2B_2C_2$ skeleton (Figure 4) of the same structural type as **I** (Scheme 1) and **C** (Scheme 2). Only one triply bridging Ru−H(B)−Ru hydrogen was found in the structure refinement. An odd number of framework hydrogen atoms is unlikely, and the ^{1}H NMR spectrum reveals the expected six framework protons, i.e., two triply bridging Ru−H(B)−Ru protons plus two B−Ht and two B−H−Ru protons. A precise mass measurement supports the presence of six framework hydrogen atoms with a molecular ion peak corresponding to $C_{28}H_{42}B_2Ru_2$, and the ^{13}C spectrum shows two framework carbon resonances of an inserted alkyne.

***nido*-1,2-(Cp*Ru)$_2$-3-CH_2CH_2Ph-4-Ph-$C_2B_2H_6$, 8**, and ***nido*-1,2-(Cp*Ru)$_2$-3-CH_2CH_2Ph-5-Ph-$C_2B_2H_6$, 9**, were isolated in yields of 3% each by a combination of column and thin-layer chromatography. The solid-state structures show that both contain a *nido*-$Ru_2B_2C_2$ framework with one fully reduced alkyne substitutent at the B(3) position (Figures 5 and 6) and only differ in the orientation of the inserted alkyne (position of Ph cage substitution). The ^{1}H spectra exhibit characteristic BC−H resonances for the inserted terminal alkynes as well as complex aliphatic CH_2 multiplets for the BCH_2CH_2Ph units. In contrast to **7**, **8** and **9** are stable to air and moisture, which suggests the terminal hydrocarbyl group present in these two compounds has a significant effect on the properties. Another

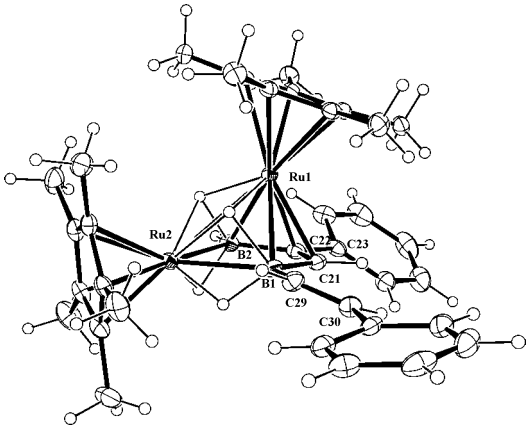

Figure 7. Molecular structure of **10**. Selected bond lengths (Å): Ru(1)−C(21), 2.1990(17); Ru(1)−C(22), 2.3725(19); Ru(1)−B(1), 2.3725(19); Ru(2)−B(1), 2.384(2); Ru(2)−B(2), 2.3876(19); B(1)−C(21), 1.537(3); B(1)−C(29), 1.573(3); B(2)−C(22), 1.556(3); C(21)−C(22), 1.414(3); C(22)−C(23), 1.495(2); C(29)−C(30), 1.336(3); Ru(1)−B(2), 2.362(2); Ru(1)−Ru(2), 2.93707(18).

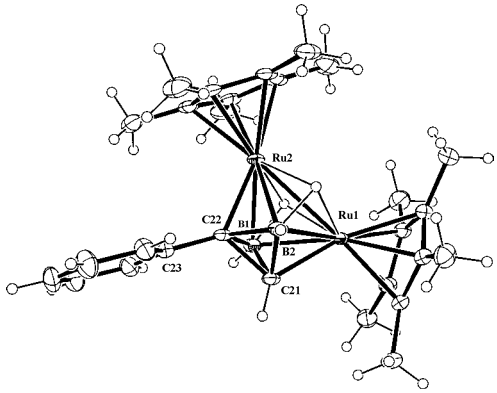

Figure 8. Molecular structure of **11**. Selected bond lengths (Å): Ru(1)−C(21), 2.071(2); Ru(1)−B(1), 2.296(3); Ru(1)−Ru(2), 2.8633(2); Ru(2)−C(22), 2.081(2); Ru(2)−B(2), 2.302(3); Ru(2)−B(1), 2.317(3); B(1)−C(21), 1.621(4); B(1)−C(22), 1.629(4); B(2)−C(21), 1.615(3); B(2)−C(22), 1.638(4); C(21)−C(22), 1.581(3); C(22)−C(23), 1.478(3); Ru(1)−B(2), 2.312(3).

curious fact is that unlike the transformation of **E** to **F** in Scheme 2, we failed to observe the conversion of **6** to **8**.

***nido*-1,2-(Cp*Ru)$_2$-3-(*trans*-CH═CHPh)-5-Ph-4,5-$C_2B_2H_6$, 10**, was isolated in a yield of 5%. The solid-state structure shows a *nido*-$Ru_2B_2C_2$ framework with a vinyl group at the B(3) position in contrast to the fully reduced alkyne found in **8/9** (Figure 7). The 1D ^{1}H spectrum reveals the characteristic BC−H signal for the inserted alkyne. Unfortunately, the two olefin protons cannot be unambiguously assigned even by ^{1}H−^{1}H COSY as their resonances overlap the phenyl group resonances. On the other hand, the ^{13}C spectrum is informative and shows characteristic broad (140.4 ppm) and sharp (138.9 ppm) resonances for a BC(H)═CH group as well as the two broad signals (110.5 and 89.2 ppm) for the inserted alkyne. We have not previously observed a vinyl substituent in this chemistry although ample precedent exists in the reactions of boranes with alkynes mediated by transition-metal complexes.[43−45] Mechanistic implications will be treated below.

Higher Temperature. The reaction at 90 °C is also complex, and five new compounds (**11**−**15**) with *closo* structures were isolated. Three of the ambient temperature *nido* products (**7**, **8**, **10**) described above were also isolated.

***closo*-4-Ph-1,2-(Cp*RuH)$_2$-4,6-$C_2B_2H_3$, 11**, was isolated in a yield of 3%. The X-ray determination reveals the same $Ru_2C_2B_2$ framework prevalent in the lower temperature reaction; however, it exhibits a *closo* octahedral structure with adjacent carbon atoms consistent with its sep count of 7 (Figure 8 and Scheme 5). The C−C bond length is ∼0.2 Å longer (C21−C22 = 1.581 Å) and the Ru−C bond distances are ∼0. 2 Å shorter (Ru1−C21 = 2.071 Å, Ru2−C22 = 2.081 Å) than those in **6**−**10**, where the inserted alkyne is on an open face of the *nido*-cluster. The ^{1}H spectrum shows one broad B−CH resonance for the inserted alkyne, two equivalent B−Ht resonances, and two equivalent triply bridging Ru−H(B)−Ru resonances. This octahedral *closo*-$Ru_2C_2B_2$ species is thermally stable and insensitive to air and moisture and is a structure type not observed from reactions of any of the other alkynes.

***closo*-1,2-(Cp*RuH)$_2$-3-CH_2CH_2Ph-5-Ph-7-CH_2CH_2Ph-4,5-$C_2B_3H_2$, 12**, was isolated in a yield of 6%. The solid-state structure in Figure 9 now shows a *closo*-$Ru_2C_2B_3$ cluster core. Two additional alkynes are incorporated into the product as

Scheme 5. Reaction Products Observed with HC≡CPh at High Temperature

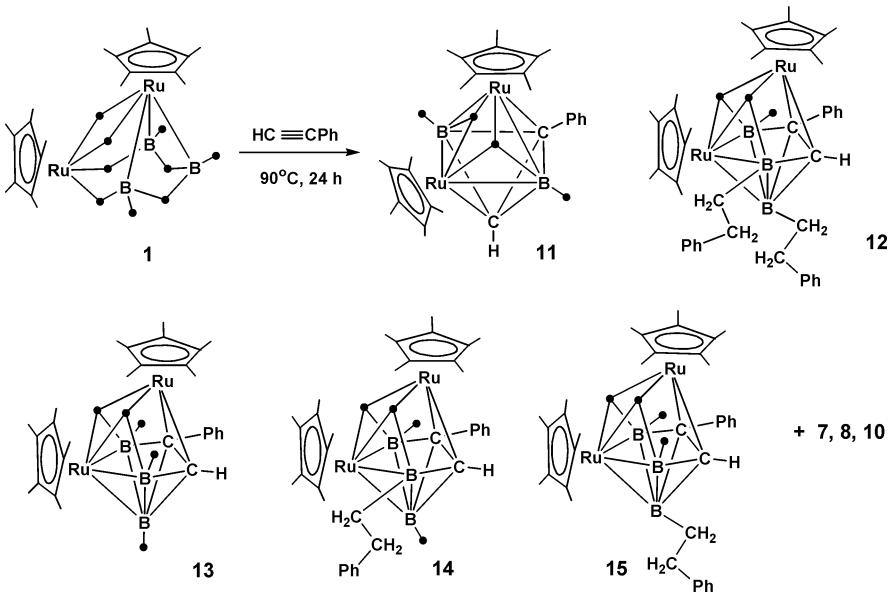

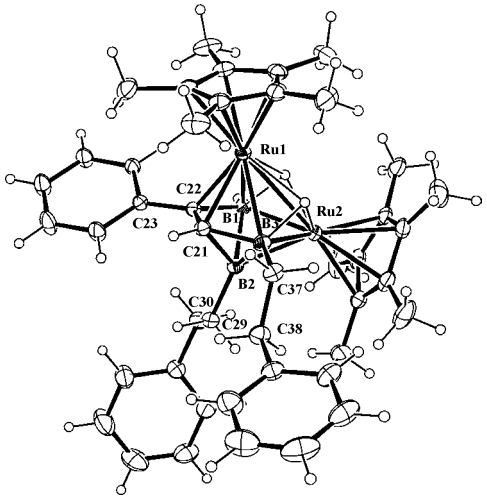

Figure 9. Molecular structure of **12**. Selected bond lengths (Å): Ru(1)−C(21), 2.1531(14); Ru(1)−C(22), 2.1763(14); Ru(1)−B(3), 2.3928(16); Ru(1)−B(1), 2.3952(16); Ru(2)−B(1), 2.1672(16); Ru(2)−B(2), 2.1884(16); B(1)−C(22), 1.563(2); B(2)−C(29), 1.596(2); B(2)−C(22), 1.803(2); B(3)−C(21), 1.566(2); C(21)−C(22), 1.4595(19); C(22)−C(23), 1.4834(19); C(29)−C(30), 1.545(2); C(37)−C(38), 1.535(2); Ru(1)−Ru(2), 2.90569(15); Ru(2)−B(3), 2.1818(16); B(1)−B(2), 1.849(2); B(2)−C(21), 1.767(2); B(2)−B(3), 1.859(2); B(3)−C(37), 1.594(2).

boron terminal substituents in equatorial and axial positions, making the cluster surface congested. The ^{1}H NMR data show resonances of one broad BC−H proton, one B−Ht proton, and two triply bridging Ru−H(B)−Ru hydrides and four sets of complex methylene multiplets. Two pairs of cross-peaks for the aliphatic CH_2 units are observed in the ^{1}H−^{1}H COSY spectrum. The ^{13}C NMR spectrum shows resonances at 91.48 ppm (B−C) and 80.68 ppm (B−CH) corresponding to inserted alkyne as well as two broad aliphatic B−CH_2 (28.15 and 25.36 ppm) and two sharp CH_2 (36.75, 33.79 ppm) resonances of the two CH_2CH_2Ph units. The previously observed conversion of **II** to **V** (Scheme 1) suggests that **12** might arise from an intermediate containing an *exo*-BH_2 fragment. If so, it does not come from **6** as heating **6** in excess of the alkyne does not lead to **12**.

***closo*-1,2-(Cp*RuH)$_2$-5-Ph-4,5-$C_2B_3H_4$, 13**, was isolated in a yield of 4%. Suitable crystals for X-ray measurement were not obtained, and its proposed structure (Scheme 5) is based on spectroscopic data. The ^{1}H NMR spectrum shows one inserted alkyne with the characteristically broad BC−H resonance at 5.49 ppm. The spectroscopic signature of a fully reduced alkyne group is not observed. Two triply bridging Ru−H(B)−Ru and three discrete B−H terminal hydrogen resonances are observed. The ^{11}B{^{1}H} NMR shows only one broad signal; however, the three different B−H terminal ^{1}H signals observed show the B−H fragments to be inequivalent. The precise mass measurement indicates a molecular ion with a formula of $C_{28}H_{41}B_3Ru_2$ consistent with the composition established by ^{1}H NMR data. Thus, a *closo*-$Ru_2C_2B_3$ framework structure is suggested. In this case **13** is the sole product when **5**, which contains a bridging BH_2 group, is heated at 90 °C for 22 h (Scheme 6).

***closo*-1,2-(Cp*RuH)$_2$-3-CH_2CH_2Ph-5-Ph-4,5-$C_2B_3H_3$, 14**, was isolated in a yield of 7%, but in the absence of single crystals its postulated structure (Scheme 5) must be based on spectroscopic data. The ^{1}H NMR spectrum reveals a broad resonance (J = 4.0 Hz) of B−CH from an inserted alkyne and two sets of complex methylene multiplets for a BCH_2CH_2Ph unit. Two types of B−Ht and two types of triply bridging Ru−H(B)−Ru resonances are observed, and one of the latter is a doublet (J = 4.0 Hz) due to coupling with the BC−H proton. The ^{13}C NMR data reveal characteristic signals for the inserted alkyne (93.42 ppm for B−C and 81.18 ppm for the B−CH) as well as the fully reduced alkyne substituent (34.18 ppm for CH_2 and 28.13 ppm for B−CH_2). The ^{11}B NMR spectrum shows two boron resonances in a ratio of 1:2. The precise mass gives a molecular ion composition of $C_{36}H_{49}B_3Ru_2$. The ^{1}H{^{11}B}−^{1}H{^{11}B} COSY spectrum does not show correlation between the BC−H and the adjacent B−Ht hydrogen atoms. This suggests BC−H may not be adjacent to a B−Ht, but it is not conclusive. Although it is clear that **14** has a *closo*- $Ru_2C_2B_3$ framework, the data are not sufficient to define the location of the hydrocarbyl unit or the orientation of the inserted alkyne.

When **6** is heated, **14** is observed as one of three products. Monitoring by NMR at 90 °C shows that **14** is dominant early, but after **6** has totally reacted in about 22 h, a new species (**15**; see below) becomes dominant (Figure 10). The conversion of **6** to **14** suggests orientation of the inserted alkyne and location

Scheme 6. Possible Rearrangement Pathways of Selected Products Derived from HC≡CPh

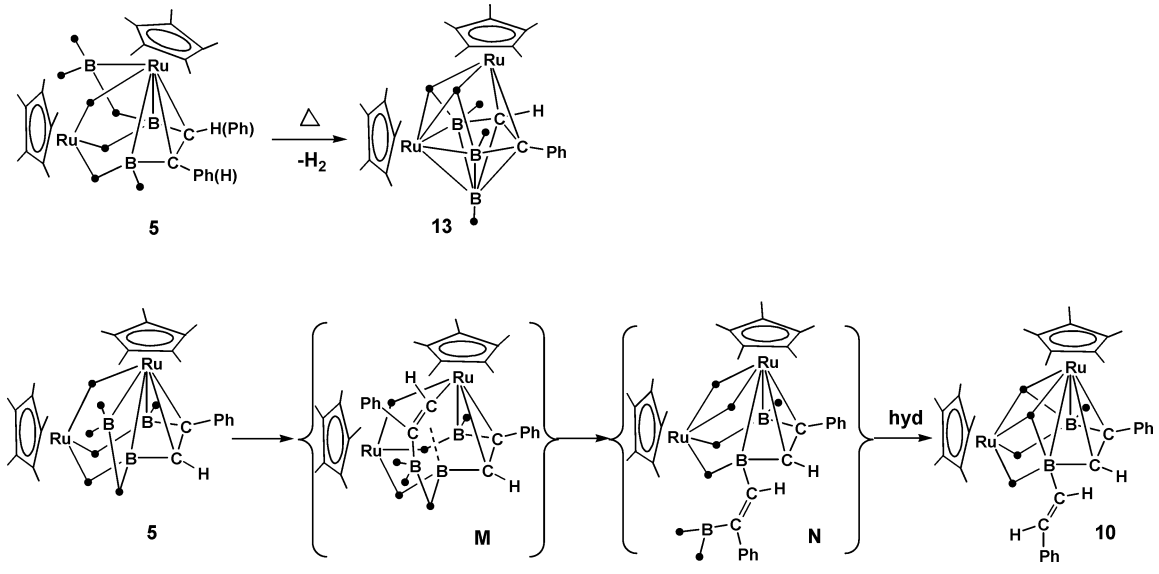

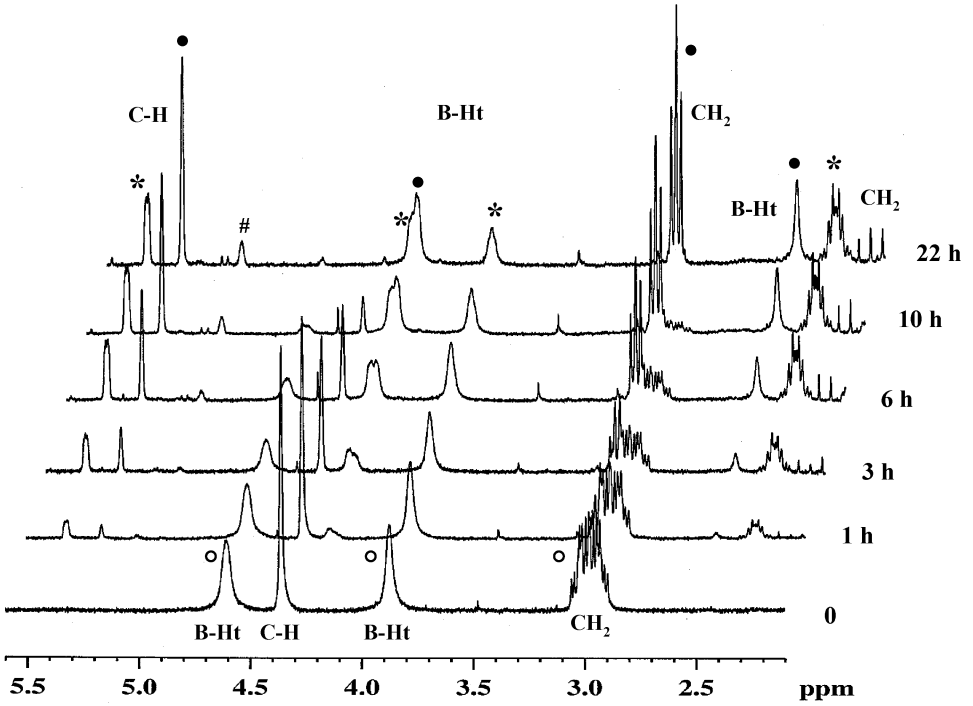

Figure 10. $^{1}H\{^{11}B\}$ NMR monitoring the conversion of **6** (○) into **14** (*) and **15** (●) at 90 °C in the region of 2−6 ppm (the pound sign represents compound **7**).

of the BCH_2CH_2Ph fragment similar to that found in **6** (Scheme 4) simply because **II** (Scheme 1) converts to crystallographically characterized structure **V** on heating. The only difference with **6** and **14** is the presence of a framework hydrocarbyl group.

***closo*-1,2-(Cp*RuH)$_2$-5-Ph-7-CH_2CH_2Ph-4,5-$C_2B_3H_3$, 15**, was isolated both from the reaction mixture (11%) and from thermolysis of **6** with the coproduct **14**. Attempts to grow crystals failed. Both ^{1}H and ^{13}C NMR data are similar to those of **14**, showing one inserted and one fully reduced alkyne. The ^{11}B NMR spectrum is also similar to that of **14**. The precise mass gives the same composition as for **14**. Hence, the spectroscopic data show **15** to be a geometrical isomer of **14**. Heating pure **14** leads to **15** with a half-life of 12 h at 84 °C (Figure 11). Hence, it is clear that **15** is a more stable isomer of **14**. What does **15** look like? It is likely that the BCH_2CH_2Ph fragment migrates into the axial B−H position (Scheme 5). Alternatively, B−C bond cleavage and R group migration is well-known in organoboron chemistry[61,62] and cannot be ruled out here. Because both ^{1}H and ^{13}C NMR data show the presence of the BC−H hydrogen, migration of the $-CH_2CH_2Ph$ group to carbon is ruled out.

Connections between Stable Products. A full sequence is **6** goes to **14** with loss of H_2 and then **14** isomerizes to **15** (Scheme 7), which parallels **5** going to **13**. One pathway for loss of an *exo*-BH_2 fragment is reinsertion to form a *closo* structure. The carbonyl oxygen of a MeOC(O)-functionalized $Ru_2C_2B_2$ framework can trap the *exo*-BH_2 and avoid cluster closure (**A**, Scheme 2). Thus, **II** and **A** yield products with complex *exo*-cluster substituents in the presence of excess alkyne

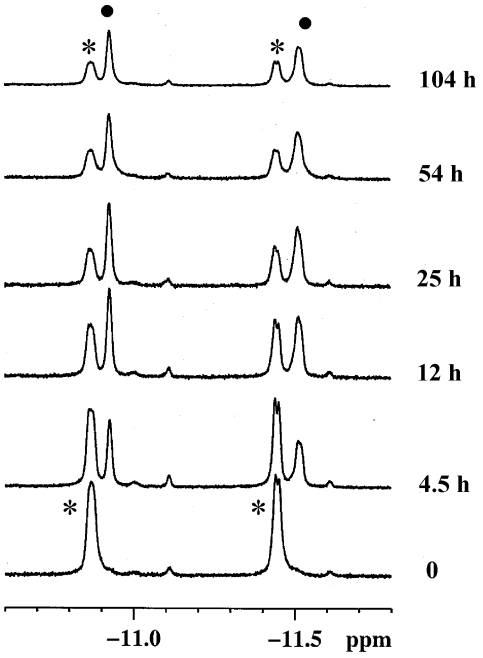

Figure 11. $^{1}H\{^{11}B\}$ NMR monitoring the conversion of **14** (*) into **15** (●) at 84 °C (only showing the high-field region for the triply bridging hydrogens Ru−H(B)−Ru) ($t_{1/2}$ = 12 h).

(Schemes 1 and 2). However, in the presence of excess of phenylacetylene **6** still generates **14** and **15**.

In all cases the thermolysis of **6** yields some **7** in an amount that varies depending on the conditions. This is analogous to the situation with **A** where **C** always appears (Scheme 2).[57] How can a hydrocarbyl group and an *exo*-cluster BH_2 unit be lost from **6** or **A** to lead to **7** or **C**? Hydrolysis during reaction or on workup is a possibility. Hence, we carried out three experiments in which differing amounts of water were introduced into C_6D_6 solutions of **6**. The results show the yield of **7** is significantly

(58) Takao, T.; Takemori, T.; Moriya, M.; Suzuki, H. *Organometallics* **2002**, *21*, 5190.
(59) Iverson, C. N.; Smith, M. R.; II, *Organometallics* **1996**, *15*, 5155.
(60) Sagawa, T.; Asano, Y.; Ozawa, F. *Organometallics* **2002**, *21*, 5879.
(61) Wrackmeyer, B. *Coord. Chem. Rev.* **1995**, *145*, 125.
(62) Crevier, T. J.; Mayer, J. M. *Angew. Chem., Int. Ed.* **1998**, *37*, 1891.

Scheme 7. Possible Reaction Pathway for Compound **6**

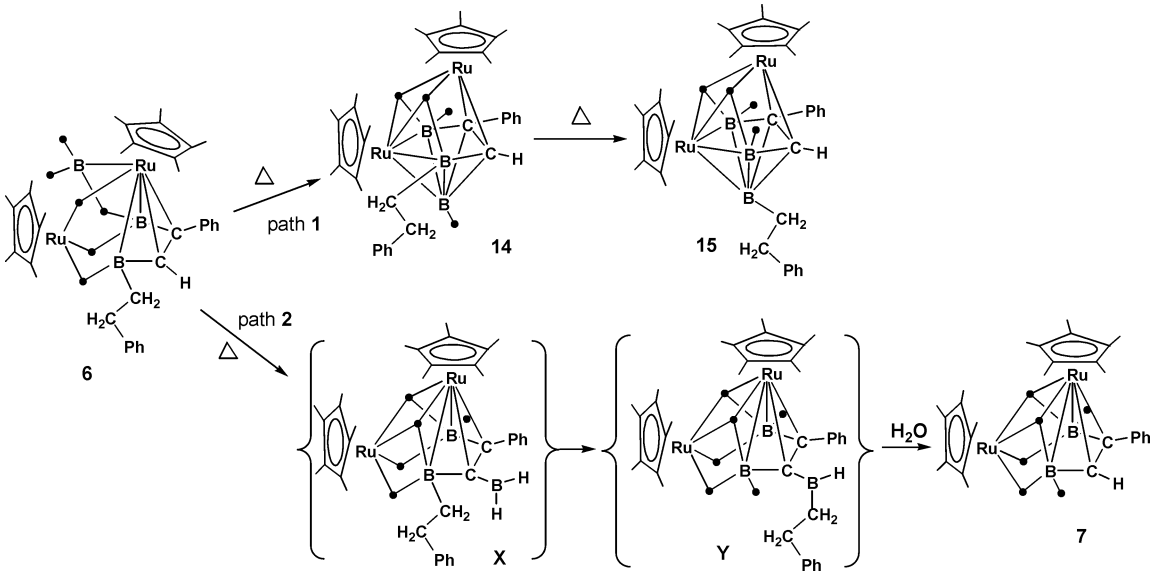

increased by added moisture. Thus, a second pathway (Scheme 7) with two intermediates, **X** and **Y**, leads to **7**, where the intermediates are based on the proposed route for the production of **D** (Scheme 2).[57] Note that **7** is one of the two major products at ambient temperature, but **6** does not react with water at ambient temperature in 1 day. Thus, the route to **7** shown in Scheme 7 is an independent route requiring both heat and moisture.

The striking difference between the products at ambient vs high temperature is the presence of *closo* compounds **11**−**15** (total of 31% yield). Some *nido* products are still observed at 90 °C (**7**, **8**, and **10** at 25%). At 90 °C the yield of **10**, which contains a vinyl group, is increased from 5% to 17%. Attempts to reduce **10** by BH_3THF at 90 °C were unsuccessful, and hence, **10** does not appear to be intermediate in the formation of **8**. A possible pathway for the formation of **10** is regioselective insertion of the alkyne into the *exo*-BH_2 unit of **5** (Scheme 6). This would generate intermediate **M** reminiscent of the insertion of an alkyne into a Pt−B bond.[59,60] Bond metathesis and skeletal hydrogen rearrangement lead to an *exo*-cluster vinyl group similar to that in **IV** (Scheme 1) albeit with a BH_2 unit (**N**). If hydrolysis of the C−BH_2 bond by adventitious moisture is more rapid than hydroboration, **10** would be generated rather than an analogue of **IV**.

In terms of stable products, the reactivity of HC≡CPh has similarities to those of both MeC≡CMe[54,55] and HC≡CCO_2Me[56,57] as well as distinct differences. In common with the other two alkynes, HC≡CPh generates μ-alkylidenes bridging Ru−B edges, cluster intermediates containing an *exo*-BH_2 unit, and *closo*-$Ru_2C_2B_3$ structures. However, **4** with a fully reduced alkyne fragment on the original cluster framework, **10** bearing a styrene group from the incomplete reduction of the alkyne, and **11** with a *closo*-$Ru_2C_2B_2$ framework are structure types not seen in the products from the other two alkynes.

Mechanistic Considerations. The variety and complexity of the ruthenacarborane products in the work described above, as well as the earlier studies with other alkynes, hide the essential features of the reaction. Are we dealing with a large set of competing reactions, or are there a few primary interactions between metallaborane and alkyne that lead to a set of consecutive reactions? If the latter situation obtains, what is the nature of the initial facile ruthenaborane−alkyne reaction, and why do we see it for ruthenaboranes but not other related metallaboranes?

Our earlier study of the reaction of **1** with HC≡CC(O)OMe was also complex, but an examination of intermediates generated at earlier reaction times showed a small number of intermediates, two of which were spectroscopically characterized. Hence, a similar study was carried out for the less reactive alkyne examined here to attempt to confirm the presence of the same two intermediates as well as to identify others. An advantage of the present work is that two of the products, **6** and **7**, account for 40% of the 70% yield of all products isolated; hence, there was the possibility of gaining a better understanding of the principal reaction pathway.

As before, we examined the reaction at early time utilizing ^{1}H NMR to monitor the evolution of intermediates and some isolated products. On the basis of characteristic abundance/time behavior, four distinct intermediates could be identified. As shown in Table 1, sufficient chemical shift data were observed to establish the framework of all four intermediates. In addition, sufficient C−H shift/coupling information was observed to define the structure of the hydrocarbyl fragments of two of the intermediates. Further, comparison of chemical shift data (Table 1) shows that the two intermediates lacking information on the hydrocarbyl fragment must be of the same type observed in the earlier study. The identification of four intermediates allows most of the isolated products in the room temperature reaction to be structurally connected to the starting materials.

Intermediate I_1. A species with a maximum in intensity at ca. 5 min (Figure 12) exhibits the set of NMR signals identified as $\mathbf{I_1}$ in Table 1 and shown in Figure 13. By comparison with the data for **1**, it is clear that the framework of **1** is retained in $\mathbf{I_1}$ albeit with loss of one RuHRu hydrogen atom and the plane of symmetry. A key resonance is that assigned to the hydrocarbyl fragment and found at δ 6.6 as a multiplet (second-order AB pattern with $\Delta\nu \approx 3$ J). Two structural possibilities exist: Ph(Ru)C═CH_2 and *trans*-H(Ru)C═CHPh. However, the former is disfavored by the 18 Hz coupling constant, and the second is only possible if the ^{1}H chemical shifts of the two protons are

Table 1. ^{1}H NMR Chemical Shifts for Intermediates in the Reaction of **1** with HC≡CPh

H type	**1** (B_n)	I_1 (B_n)	I_2 (B_n)	I_3 (B_n)	I_4 (B_n)	A
B−H	2.7 (1)	2.6 (1)	2.6 (1)	2.5 (1)	2.3 (1)	3.06
B−H	2.7 (2)	2.7 (2)	2.9 (3)	3.0 (2)	5.4 (2)	3.09
B−H	3.3 (3)	3.2 (3)	3.1 (3)	3.5 (3)	3.2 (3)	4.60
B−H−B	−4.0 (4)	−3.3 (4)	−4.3 (5)	−1.8 (4)	0.0 (4)	−1.2 q
B−H−B	−4.0 (5)	−4.6 (5)	−4.4 t (4)	−1.9 (5)	0.0 (5)	−1.9 t
B−H−Ru	−11.2 (6)	−10.0 (6)	−11.2 t (6)	−11.0 (7)	−6.3 (6)	−10.8 t
B−H−Ru	−11.2 (7)	−12.7 (7)		−15.8 d (6)	−11.7 t (7)	−16.2 d
B−H−Ru					−12.4 (8)	
Ru−H−Ru	−13.6 (8)	−12.8 (8)	−10.9 (8)	−21.2 (8)		−21.3
Ru−H−Ru	−13.6 (9)		−8.8 d (9)			
C−H		6.6 m (9)	?	?	3.8 d (9)	
C−H		6.6 m (10)	?	?	3.4 d (10)	
Cp*	1.92	1.87	1.65	1.40	1.83	1.55
Cp*	1.78	1.86	1.825	1.77	1.74	1.75

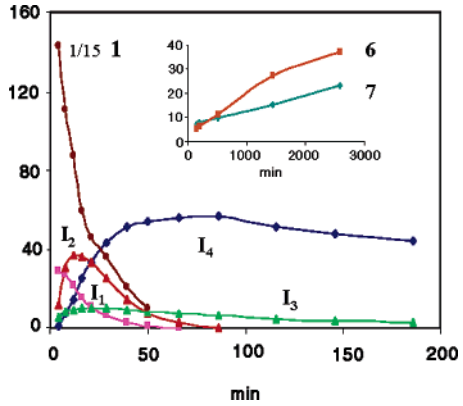

Figure 12. Abundance of early intermediates showing the loss of **1** and the formation of the two major products **6** and **7** (inset) on a reduced scale.

approximately equal. Justification for similar proton chemical shifts in the second case comes from the NMR behavior of compound **10** for which a solid-state structure is available. As shown in Scheme 4, **10** exhibits the same type of fragment postulated for $\mathbf{I_1}$, albeit bound to B rather than Ru, with proton resonances at $\delta = 7.1-7.2$. Generation of $\mathbf{I_1}$ by hydroruthenation rather than hydroboration is consistent with the loss of a metal hydride. It is also supported by the similarity in line widths of the C−H proton signals relative to those of, e.g., compound **4**, where the boron atom bound to the carbon atom substantially broadens the hydrogen resonances. The time dependences in the abundances of $\mathbf{I_1}$ and **3** rule out the direct generation of **3** from $\mathbf{I_1}$. The existence of another intermediate, possibly the 2,3-isomer of **3** shown in Figure 13, is required. If so, hydroruthenation takes place at the basal ruthenium site, which is logical given that it is adjacent to the open face of the square pyramidal cluster. Subsequent hydroboration followed by rearrangement leads to **3**.

Intermediate $\mathbf{I_4}$. The second intermediate for which a complete set of ^{1}H data are available, $\mathbf{I_4}$, has a broad maximum in abundance at about 80 min (Figure 12). Comparison of the resonances associated with the framework with those of **1** shows that the framework bonding has been perturbed. Comparison with, e.g., **6** suggests that insertion of the alkyne has taken place. The hydrocarbyl resonances, a doublet of doublets centered at $\delta = 3.6$, rule out some possibilities and suggest a reasonable structure. Again there are two acceptable assignments:

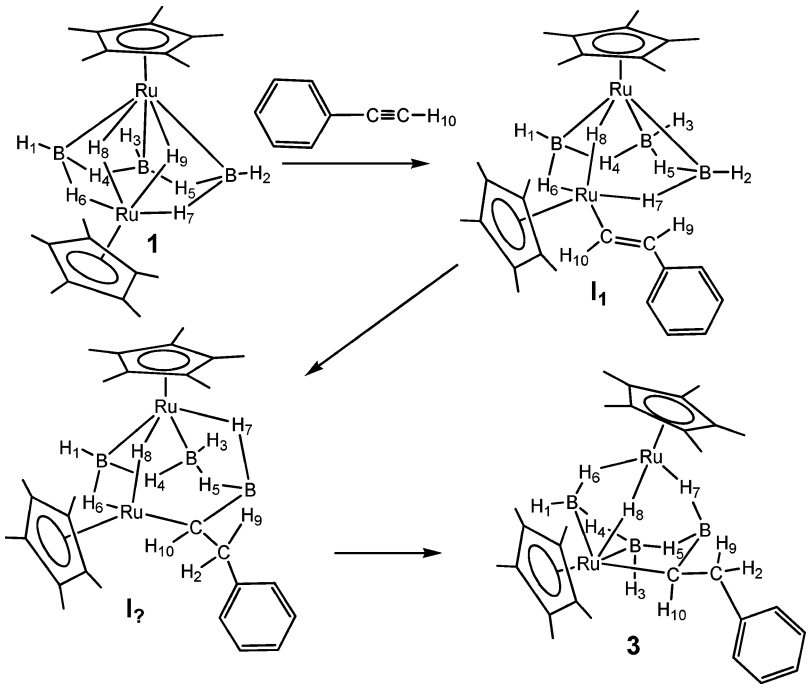

Figure 13. Pathway for the formation of **3** from **1** via observed intermediate $\mathbf{I_1}$ and postulated intermediate $\mathbf{I_?}$.

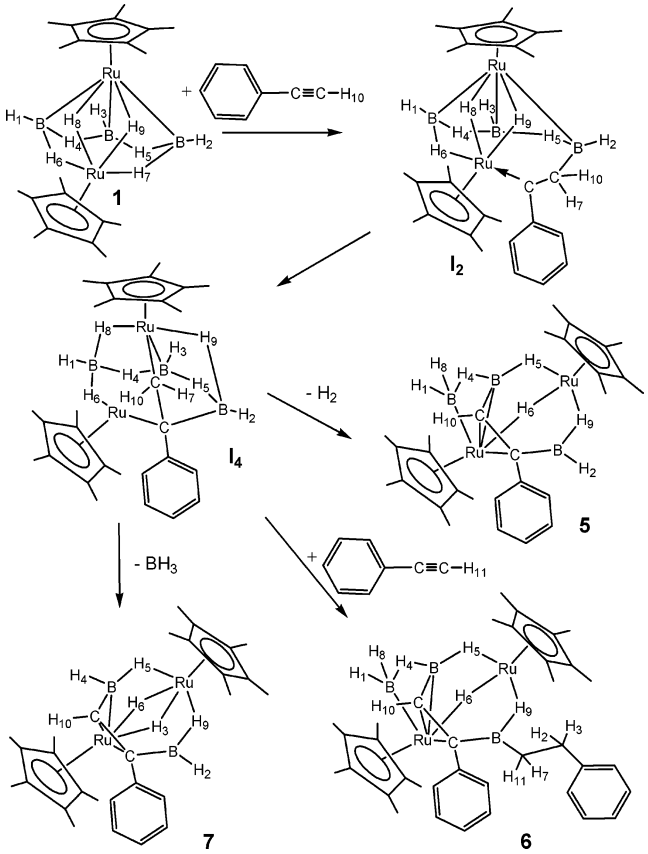

Figure 14. Pathway for the formation of **5**−**7** from **1** via observed intermediates $\mathbf{I_2}$ and $\mathbf{I_4}$.

(X)(Y)(Ph)C−CH_2(Z) or (X)(Ph)(H)C−C(H)(Y)(Z). Neither doublet shows sufficient broadening to permit a B−C−H linkage, thereby ruling out Z = B in the first case and any connection to B in the second. Considering the structures of **6** and **7**, the second situation appears ruled out altogether. The observed coupling constant (11 Hz) is low for geminal coupling but not impossible. Hence, the first assignment with Z = Ru is judged most likely.

The preferred structure for $\mathbf{I_4}$ is shown in Figure 14, but clearly others can be generated to fit the available shift data. This preference is based on two additional factors. First, the structure adopted for $\mathbf{I_4}$ leads to the frameworks of the products **6**, **7**, and **5** (minor) by addition of PhC≡CH, loss of BH_3, and loss of H_2, respectively. Note that product type **5** is a major product for 2-butyne. Addition of the internal alkyne to yield **6** may no longer be competitive with H_2 loss. Second, the time/abundance observations suggest that $\mathbf{I_4}$ is generated from $\mathbf{I_2}$, which in turn is generated from **1** (see immediately below).

One potential source of doubt of the assignment comes from the fact that the abundance of $\mathbf{I_4}$ remains significant even after 8 h in the NMR tube. Hence, one might well wonder why it is not observed as a product. First, the NMR scale reaction is not effectively stirred, and as pointed out above, the abundances of some reaction products were modified by the necessarily slow chromatographic procedures; i.e., it is possible that the yield of **7** is enhanced at the expense of $\mathbf{I_4}$ by removal of BH_3 from $\mathbf{I_4}$ on the silica column material.

Intermediates $\mathbf{I_2}$ and $\mathbf{I_3}$. Intermediates $\mathbf{I_2}$ and $\mathbf{I_3}$ seem to pose intractable structural problems as the signals from hydrocarbyl fragments were not identified. Most likely they are hidden in the most complex region of the spectrum. But as noted above, the framework resonances of $\mathbf{I_2}$ and $\mathbf{I_3}$ have chemical shifts nearly identical to those exhibited by intermediates **B** and **A** in the HC≡CC(O)OMe reaction (the data for **A** are included in Table 1). A good assignment for **A** resulted from a good fit of a second-order ABX pattern in the δ 2 region; hence, the same type of framework-bound, carbene-bridging ligand structure is postulated for $\mathbf{I_2}$ (boron-bound) and $\mathbf{I_3}$ (ruthenium-bound); i.e., they are cluster isomers. As shown in Figure 15, $\mathbf{I_3}$ easily leads to **2** with the observed regiochemistry, and (Figure 14) $\mathbf{I_2}$ connects **1** and $\mathbf{I_4}$. The time dependence of $\mathbf{I_2}$ is consistent with it being intermediate to $\mathbf{I_4}$. The difference between $\mathbf{I_2}$ and $\mathbf{I_3}$

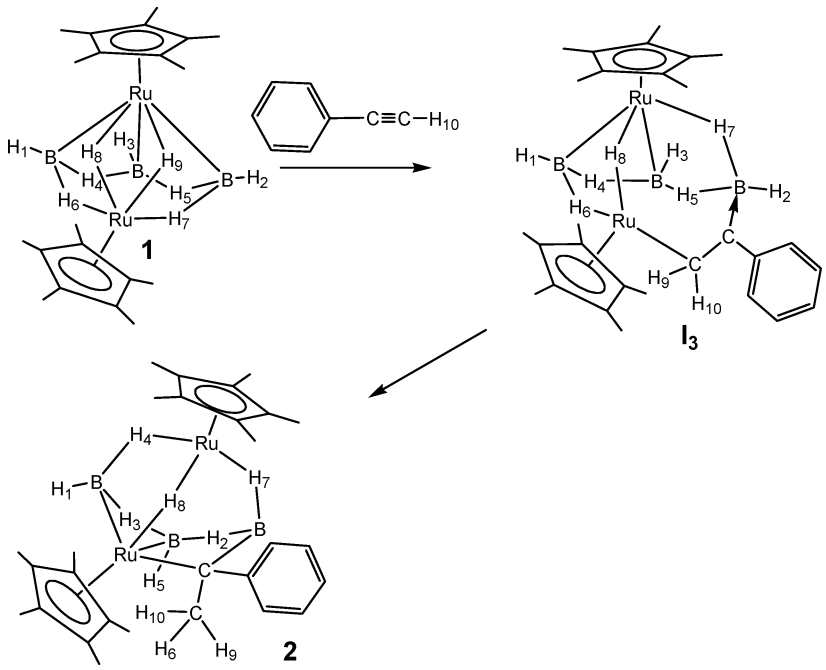

Figure 15. Pathway for the formation of **2** from **1** via observed intermediate $\mathbf{I_3}$.

would appear to be B−H−Ru hydrometalation vs hydroruthenation. Caution is necessary as the hydrogen atom type missing in the structure of the intermediate need not be the same hydrogen type on **1** that reacts simply because skeletal hydrogen rearrangements can be fast. In fact, both may result from hydroruthenation, with $\mathbf{I_2}$ being the more stable isomeric form.

In summary, reasonable pathways to isolated products **2**, **3**, and **5**−**7** exist, and small variants easily account for **8**−**10** as well. From all of this detail comes one strong conclusion which supplies an answer to the question posed at the beginning of this section. It is facile hydrometalation that is the key to the reactivity of the hydrogen-rich diruthenaborane with alkynes. The two extra Ru−H−Ru bridges necessary to meet the electron count for a *nido* square pyramidal framework is a structural feature that distinguishes this compound from most of the other related metallaboranes we have synthesized. Hydroruthenation plays a major role, but most likely, the available borane hydrogens play a role as well even if a subsidiary one.

Of particular importance to this argument identifying the alkyne reactivity with extra Ru−H on the ruthenaborane framework is the fact that the isolectronic and cluster isostructural Rh analogue of **1**, *nido*-1,2-$(Cp^*Rh)_2B_3H_7$, yields alkyne cyclotrimerization as the primary reaction route. Other related metallaboranes with earlier transition metals, when treated with alkynes, have not reacted at all. These metallaboranes of the earlier metals are effectively "hydrogen-poor" and often adopt more condensed structures, but even those with more open structures are ineffective reaction partners for alkynes.

Conclusions

The Ru−H−Ru hydrides on the framework of *nido*-1,2-$(Cp^*RuH)_2B_3H_7$ leads to facile reaction with alkynes with a variety of substituents. Three primary hydroruthenation adducts are formed from which more stable organo-substituted ruthenaboranes and ruthenacarboranes evolve, the variety of which depends on the number of substituents (internal or terminal alkyne) and the properties of the alkyne substituents. One isolable product type under mild conditions contains an *exo*-cluster BH_2 species. Extrusion of a borane vertex on alkyne insertion appears to be a general mechanistic feature that can be followed by reincorporation forming either *closo*- or *nido*-clusters or by loss to yield diboron clusters. Although useful control of reactivity has not been established, sufficient parameters remain to be optimized to suggest yields of selected products greater than the 20−30% observed are possible. The cooperative activity of Ru−H and B−H fragments suggests that metallaboranes can become a new reaction tool for the manipulation of selected organic substrates.

Experimental Section

General Procedures. All operations were conducted under an argon atmosphere using standard Schlenk techniques. Solvents were dried with appropriate reagents and distilled before use under N_2. $LiBH_4$ (2 M in THF), HC≡CPh (Aldrich), and [$(Cp^*RuCl_2)n$] (Strem) were used as received. *nido*-1,2-$(Cp^*Ru)_2B_3H_9$[3] was prepared according to the literature procedures. Silica gel (ICN 32-63, 60 Å) was purchased from ICN Biomedicals GmbH and predried at 180 °C before use. NMR spectra were recorded on a Bruker AMX 400 or a Varian 500 FT-NMR spectrometer. Residual proton signals of solvents were used as reference: ^{1}H (δ, ppm, benzene-d_6, 7.16) and ^{13}C (δ, ppm, benzene-d_6, 128.39). For ^{11}B an external reference was used: a sealed capillary containing [$(Me_4N)(B_3H_8)$] in acetone-d_6 (δ, ppm, −29.7). Infrared spectra were measured on a Perkin-Elmer Paragon 1000 FT-IR spectrometer. Mass spectra were obtained on a JEOL LMS-AX505 spectrometer using the EI or FAB ionization modes.

Synthesis of 2−10. To the orange solution of **1** (200 mg, 0.39 mmol) in hexanes (20 mL) was added PhC≡CH (0.5 mL, 4.60 mmol). The resulting mixture was stirred for 7 h at ambient temperature. After removal of solvent the residue was chromatographed on silica gel. Elution with hexane/toluene (30:1) gave **2** (8.0 mg, 3.3%), elution with hexane/toluene (10:1) gave **3** (12.6 mg, 5.2%) and **4** (21.5 mg, 8.9%), elution with hexane/toluene (8:1) gave **5** (11.2 mg, 4.7%) and **6** (53.2 mg, 18.9%), elution with hexane/toluene (6:1) gave 7 (47.5 mg, 20.1%) and **8** (9.4 mg, 3.4%), and elution with hexane/toluene (3:1) gave **9** (14.3 mg, 3.1%) and **10** (8.7 mg, 5.2%).

Data for 2. ^{1}H{^{11}B} (C_6D_6): δ 7.660 (m, 2H, Ph), 7.178 (m, 2H, Ph), 7.063 (m, 1H, Ph), 3.727 (s, br, 2H, B−Ht), 1.733 (s, 15H, Cp*), 1.651 (s, 15H, Cp*), 1.639 (s, 3H, Me), −2.631 (s, br, 1H, B−H−B), −2.751 (s, br, 1H, B−H−B), −11.146 (s, br, 1H, B−H−Ru), −11.286 (s, 1H, br, B−H−Ru), −15.429 (s, 1H, Ru−H−Ru). ^{11}B{^{1}H} (C_6D_6): δ 19.17, 15.58, 9.62 (1:1:1). IR (KBr): ν (cm^{-1}) 2512 and 2430 (B−H). MS (70 eV): *m*/*z* (rel intens) [M^+ − H] (35), calcd 617.1809 for $C_{28}H_{44}B_3Ru_2$, found 617.1791.

Data for 4. ^{1}H{^{11}B} (C_6D_6): δ 7.306 (m, 2H, Ph), 7.232 (m, 2H, Ph), 7.097 (m, 1H, Ph), 3.093 (s, br, 1H, B−Ht), 2.800 (m, 2H, CH_2), 2.326 (s, br, 1H, B−Ht), 1.921 (s, 15H, Cp*), 1.829 (s, 15H, Cp*), 1.397 (m, 2H, CH_2), −2.936 (s, br, 1H, B−H−B), −4.782 (s, br, 1H, B−H−B), −10.179 (s, br, 1H, B−H−Ru), −11.755 (s, br, 1H, B−H−Ru), −13.394 (s, br, 1H, Ru−H(B)−Ru), −13.502 (s, 1H, Ru−H−Ru). ^{13}C (C_6D_6): δ 146.82, 128.96, 128.77, 125.92 (Ph), 97.04, 84.74 (Cp*), 39.73 (CH_2), 26.09 (br, B−CH_2), 12.61, 11.91 (Cp*). ^{11}B{^{1}H} (C_6D_6): δ 3.95, −4.45, −6.09 (1:1:1). IR (KBr): ν (cm^{-1}) 2502 and 2465 (B−H). MS (70 eV): *m*/*z* (rel intens) [M^+ − 2H] (20), calcd 618.1887 for $C_{28}H_{45}B_3Ru_2$, found 618.1889.

Data for 5. ^{1}H{^{11}B} (C_6D_6): δ 7.800 (m, 2H, Ph), 7.194 (m, 2H, Ph), 7.096 (m, 1H, Ph), 4.786 (s, br, 1H, CH), 4.676 (s, br, 1H, B−Ht), 3.841 (s, br, 2H, B−Ht), 1.822 (s, 15H, Cp*), 1.466 (s, 15H, Cp*), −2.428 (q, J = 7 Hz, 1H, B−H−B), −10.467 (s, br, 1H, B−H−Ru), −14.285 (s, 1H, Ru−H−Ru), −14.793 (s, br, 1H, B−H−Ru). ^{11}B{^{1}H} (C_6D_6): δ 23.64, 20.99, 13.94 (1:1:1). IR (KBr): ν (cm^{-1}) 2508, 2427 (B−H). MS (70 eV): *m*/*z* (rel intens) [M^+] (70), calcd 616.1731 for $C_{28}H_{43}B_3Ru_2$, found 616.1752.

Data for 6. ^{1}H{^{11}B} (C_6D_6): δ 7.742 (m, 2H, Ph), 7.472 (m, 2H, Ph), 7.309 (m, 2H, Ph), 7.193−7.110 (4H, Ph), 4.599 (s, br, 1H, B−Ht), 4.357 (s, 1H, CH), 3.867 (s, br, 1H, B−Ht), 2.976 (m, 2H, CH_2), 1.357 (m, 2H, CH_2), 1.809 (s, 15H, Cp*), 1.361 (s, 15H, Cp*), −2.350 (s, br, 1H, B−H−B), −10.742 (s, br, 1H, B−H−Ru), −14.661(s, 1H, Ru−H−Ru), −15.133 (s, br, 1H, B−H−Ru). ^{13}C (C_6D_6): δ 147.41, 142.08, 129.01, 128.89, 128.31, 127.45, 126.98, 125.95 (Ph), 93.88, 89.25 (Cp*), 88.63 (br, B−CH), 37.10 (CH_2), 29.68 (br, B−CH_2), 12.02, 10.22 (Cp*). ^{11}B{^{1}H} (C_6D_6): δ 28.66, 23.64, 13.94 (1:1:1). IR (KBr): ν (cm^{-1}) 2481, 2436 (B−H). MS (70 eV): *m*/*z* (rel intens) [M^+] (100), calcd 720.2357 for $C_{36}H_{51}B_3Ru_2$, found 720.2391.

Data for 7. ^{1}H{^{11}B} (C_6D_6): δ 7.894 (m, 2H, Ph), 7.170 (m, 2H, Ph), 7.089 (m, 1H, Ph), 4.991 (s, br, 1H, B−CH), 2.697 (t, J = 6.0 Hz, 1H, B−Ht), 2.272 (t, J = 6.0 Hz, 1H, B−Ht), 1.858 (s, 15H, Cp*), 1.587 (s, 15H, Cp*), −11.386 (t, J = 6.0 Hz, 1H, Ru−H(B)−Ru), −11.447 (t, J = 6.0 Hz, 1H, Ru−H(B)−Ru), −11.942 (t, J = 6.0 Hz, 1H, B−H−Ru), −12.465 (t, J = 6.0 Hz, 1H, B−H−Ru). ^{13}C (C_6D_6): δ 146.94, 129.00, 127.99, 125.74 (Ph), 111.36 (br, B−C), 91.89 (Cp*), 91.89 (br, B−CH), 87.47 (Cp*), 12.34, 11.14 (Cp*). ^{11}B{^{1}H} (C_6D_6): δ −13.04, −16.67 (1:1). IR (KBr): ν (cm^{-1}) 2445, 2426 (B−H). MS (70 eV): *m*/*z* (rel intens) [M^+] (20), calcd 604.1560 for $C_{28}H_{42}B_2Ru_2$, found 604.1575.

Data for 8. ^{1}H{^{11}B} (C_6D_6): δ 7.872 (m, 2H, Ph), 7.510 (m, 2H, Ph), 7.318 (m, 2H, Ph), 7.209 (m, 2H, Ph), 7.157 (m, 1H, Ph), 7.105 (m, 1H, Ph), 4.626 (s, br, 1H, B−CH), 3.125 (m, 2H, CH_2), 2.622 (t,

Table 2. Crystallographic Data and Structure Refinement Information for **2**, **4**, and **6**−**8**

	2	4	6	7	8
emirical formula	$C_{28}H_{45}B_3Ru_2$	$C_{28}H_{47}B_3Ru_2$	$C_{36}H_{51}B_3Ru_2$	$C_{28}H_{42}B_2Ru_2$	$C_{36}H_{50}B_2Ru_2$
fw	616.21	618.23	718.34	602.38	706.52
cryst syst	monoclinic	orthorhombic	monoclinic	orthorhombic	monoclinic
space group	*P*2(1)/*c*	$P2_12_12_1$	*P*2(1)/*c*	*Pna*2(1)	Pc
a (Å)	19.5340(5)	8.5992(4)	11.60190(10)	23.5289(14)	17.2749(2)
b (Å)	8.5747(2)	17.5873(7)	26.6818(3)	8.3396(4)	11.4652(1)
c (Å)	17.2984(5)	18.7960(8)	11.73530(10)	13.4889(7)	17.4982(2)
α (deg)	90	90	90	90	90
β (deg)	109.896(2)	90	114.6280(10)	90	106.880(1)
γ (deg)	90	90	90	90	90
V (Å^3)	2724.51(12)	2842.6(2)	3302.31(5)	2646.8(2)	3316.38(6)
Z	4	4	4	4	4
D_{calcd} (g/cm^3)	1.502	1.445	1.445	1.512	1.415
F(000)	1264	1272	1480	1232	1456
μ (mm^{-1})	1.123	1.077	0.938	1.155	0.933
cryst size (mm)	0.2 × 0.11 × 0.07	0.33 × 0.19 × 0.04	0.24 × 0.07 × 0.06	0.28 × 0.2 × 0.01	0.3 × 0.16 × 0.09
θ range (deg)	1.11−33.03	1.59−30.50	2.06−31.57	1.73−28.28	2.16−34.45
min and max trans	0.9285, 0.8049	0.9582, 0.7177	0.9450, 0.8034	0.9885, 0.7381	0.9249, 0.7671
no. of reflns collected	41352	27760	67169	21740	60471
no. of unique reflns (R_{int})	10232 (0.0384)	8315 (0.0383)	10988 (0.0534)	5891 (0.0693)	23382 (0.0342)
no. of data/restraints/params	10232/0/337	8315/0/319	10988/0/408	5891/1/306	23382/2/782
GOF	1.021	1.060	1.044	1.037	0.994
R indices ($I > 2\sigma(I)$)	R1 = 0.0308	R1 = 0.0420	R1 = 0.0283	R1 = 0.0497	R1 = 0.0282
	wR2 = 0.0736	wR2 = 0.1057	wR2 = 0.0567	wR2 = 0.1123	wR2 = 0.0580
R indices (all data)	R1 = 0.0409	R1 = 0.0503	R1 = 0.0451	R1 = 0.0604	R1 = 0.0344
	wR2 = 0.0792	wR2 = 0.1115	wR2 = 0.0601	wR2 = 0.1172	wR2 = 0.0595
largest diff peak and hole (e/Å^3)	1.852, −0.777	2.924, −1.152	0.775, −0.610	2.323, −1.259	0.828, −0.656

J = 7.0 Hz, 1H, B−Ht), 1.856 (s, 15H, Cp*), 1.512 (s, 15H, Cp*), 1.502 (m, 2H, CH_2), −11.290 (s, br, 1H, Ru−H(B)−Ru), −11.912 (s, br, 1H, Ru−H(B)−Ru), −12.134 (s, br, 1H, B−H−Ru), −12.803 (s, br, 1H, B−H−Ru). ^{13}C (C_6D_6): *δ* 147.68, 146.73, 129.02, 129.00, 128.70, 128.03, 125.88, 125.80 (Ph), 91.70 (Cp*), 90.36 (br, B−CH), 87.57 (Cp*), 38.98 (CH_2), 25.05 (br, B−CH_2), 12.40, 11.02 (Cp*). ^{11}B{^{1}H} (C_6D_6): *δ* −1.24, −17.11 (1:1). IR (KBr): *ν* (cm^{-1}) 2431 (B−H). MS (70 eV): *m*/*z* (rel intens) [M$^+$] (50), calcd 708.2186 for $C_{36}H_{50}B_2Ru_2$, found 708.2153.

Data for 9. ^{1}H{^{11}B} (C_6D_6): *δ* 7.739 (m, 2H, Ph), 7.407 (m, 2H, Ph), 7.282 (m, 2H, Ph), 7.231 (m, 2H, Ph), 7.132−7.000 (2H, Ph), 4.756 (s, br, 1H, B−CH), 2.822 (m, 2H, CH_2), 2.167 (s, br, 1H, B−Ht), 1.939 (m, 2H, CH_2), 1.841 (s, 15H, Cp*), 1.630 (s, 15H, Cp*), −11.383 (s, br, 2H, Ru−H(B)−Ru), −12.364 (s, br, 1H, B−H−Ru), −12.615 (s, br, 1H, B−H−Ru). ^{11}B{^{1}H} (C_6D_6): *δ* −7.02, −13.58 (1:1). IR (KBr): *ν* 2434 (B−H). MS (70 eV): *m*/*z* (rel intens) [M$^+$] (100), calcd 708.2186 for $C_{36}H_{50}B_2Ru_2$, found 708.2219.

Data for 10. ^{1}H{^{11}B} (C_6D_6): *δ* 7.898 (m, 2H, Ph), 7.716 (m, 2H, Ph), 7.317 (m, 2H, Ph), 7.234−7.112 (4H of Ph and 2H of CH═CH overlapping), 4.892 (s, br, 1H, B−CH), 2.676 (t, J = 6.0 Hz, 1H, B−Ht), 1.885 (s, 15H, Cp*), 1.505 (s, 15H, Cp*), −11.148 (s, br, 1H, Ru−H(B)−Ru), −11.321 (s, br, 1H, Ru−H(B)−Ru), −12.030 (t, J = 6.0 Hz, 1H, B−H−Ru), −12.062 (t, J = 6.0 Hz, 1H, B−H−Ru). ^{13}C (C_6D_6): *δ* 146.68, 141.29 (Ph), 140.36 (br, B−CH═), 138.86 (═CH), 129.36, 128.70, 128.04, 127.14, 126.50, 125.84 (Ph), 110.45 (br, C−B), 92.17 (Cp*), 89.24 (br, B−CH), 88.15 (Cp*), 12.44, 10.98 (Cp*). ^{11}B{^{1}H} (C_6D_6): *δ* −3.50, −16.52 (1:1). IR (KBr): *ν* (cm^{-1}) 2453, 2447, 2433 (B−H). MS (70 eV): *m*/*z* (rel intens) [M$^+$] (30), calcd 706.2029 for $C_{36}H_{48}B_2Ru_2$, found 706.2012.

Synthesis of 11−**15.** To the orange solution of **1** (240 mg, 0.46 mmol) in toluene (20 mL) was added PhC≡CH (0.8 mL, 7.42 mmol). The resulting mixture was stirred for 24 h at 90 °C. After removal of solvent the residue was chromatographed on silica gel. Elution with hexane/toluene (30:1) gave **11** (7 mg, 2.5%) in pink, elution with hexane/toluene (15:1) gave **13** (10.5 mg, 3.7%) in yellow, elution with hexane/toluene (6:1) gave **15** (36 mg, 10.9%) and **14** (23 mg, 7.0%), elution with hexane/toluene (4:1) gave **12** (23.3 mg, 6.2%), elution with hexane/toluene (3:1) gave **7** (14.7 mg, 5.3%) and **8** (10.6 mg, 3.3%), and elution with hexane/toluene (2:1) gave **10** (54.8 mg, 16.9%).

Data for 11. ^{1}H{^{11}B} (C_6D_6): *δ* 7.562 (m, 2H, Ph), 7.142 (m, 2H, Ph), 7.082 (m, 1H, Ph), 4.802 (s, br, 1H, B−CH), 1.954 (s, 15H, Cp*), 1.794 (s, 15H, Cp*), 1.664 (br, 2H, B−Ht), −11.816 (s, br, 2H, Ru−H(B)−Ru). ^{11}B (C_6D_6): *δ* −19.80 (J = 120 Hz). IR (KBr): *ν* (cm^{-1}) 2530, 2521 (B−H). MS (70 eV): *m*/*z* (rel intens) [M$^+$] (100), calcd 602.1403 for $C_{28}H_{40}B_2Ru_2$, found 602.1434.

Data for 12. ^{1}H{^{11}B} (C_6D_6): *δ* 7.826 (m, 2H, Ph), 7.545 (m, 2H, Ph), 7.346 (m, 2H, Ph), 7.251 (m, 2H, Ph), 7.100 (m, 2H, Ph), 7.002 (m, 2H, Ph) (3 *para* protons are underneath the above peaks), 5.314 (s, br, 1H, B−CH), 4.290 (s, br, 1H, B−Ht), 3.076 (m, 2H, CH_2), 2.270 (m, 1H, CH_2), 2.188 (m, 1H, CH_2), 2.002 (s, 15H, Cp*), 1.841 (m, 2H, CH_2), 1.566 (s, 15H, Cp*), 0.559 (m, 2H, CH_2), −11.200 (s, br, 1H, Ru−H(B)−Ru), −11.523 (s, br, 1H, Ru−H(B)−Ru). ^{13}C (C_6D_6): *δ* 147.55, 147.37, 146.60, 129.45, 129.16, 128.77, 128.68, 127.06, 126.08, 125.69(Ph), 95.07 (Cp*), 91.48 (br, B−C), 86.97 (Cp*), 80.68 (br, B−CH), 36.75 (CH_2) 33.79 (CH_2), 28.15 (B−CH_2), 25.36 (B−CH_2), 12.16, 11.45 (Cp*). ^{11}B{^{1}H} (C_6D_6): *δ* 16.21, 9.79 (2:1). IR (KBr): *ν* (cm^{-1}) 2477(B−H). MS (70 eV): *m*/*z* (rel intens) [M$^+$] (5), calcd 822.2826 for $C_{44}H_{57}B_3Ru_2$, found 822.2829.

Data for 13. ^{1}H{^{11}B} (C_6D_6): *δ* 7.757 (m, 2H, Ph), 7.159 (m, 2H, Ph), 7.109 (m, 1H, Ph), 5.492 (d, br, J = 5.0 Hz, 1H, B−CH), 4.206 (d, br, J = 5.0 Hz, 1H, B−Ht), 3.941 (t, br, J = 5.0 Hz, 1H, B−Ht), 2.456 (s, br, 1H, B−Ht), 2.072 (s, 15H, Cp*), 1.611 (s, 15H, Cp*), −10.643 (br, 1H, Ru−H(B)−Ru), −11.343 (d, br, J = 5.0 Hz, 1H, Ru−H(B)−Ru). ^{11}B{^{1}H} (C_6D_6): *δ* 10.12. IR (KBr): *ν* (cm^{-1}) 2487, 2472 (B−H). MS (70 eV): *m*/*z* (rel intens) [M$^+$] (5), calcd 614.1574 for $C_{28}H_{41}B_3Ru_2$, found 614.1588.

Data for 14. ^{1}H{^{11}B} (C_6D_6): *δ* 7.778 (m, 2H, Ph), 7.218 (m, 2H, Ph), 7.142−7.057 (m, 6H, Ph), 5.416 (d, br, J = 4.0 Hz, 1H, B−CH), 4.231 (s, br, 1H, B−Ht), 3.867 (s, br, 1H, B−Ht), 2.323 (m, 2H, CH_2), 2.064 (s, 15H, Cp*), 1.590 (s, 15H, Cp*), 0.511 (m, 2H, CH_2), −10.865 (s, br, 1H, Ru−H(B)−Ru), −11.437 (d, br, J = 4.0 Hz, 1H, Ru−H(B)−Ru). ^{13}C (C_6D_6): *δ* 146.43, 140.00, 129.58, 128.74, 128.69, 128.55, 127.03, 125.70 (Ph), 94.23 (Cp*), 93.42 (br, B−C), 87.20 (Cp*), 81.18 (br, B−CH), 34.18 (CH_2), 28.13 (B−CH_2), 12.20, 11.49 (Cp*). ^{11}B{^{1}H} (C_6D_6): *δ* 16.73, 9.09 (1:2). IR (KBr): *ν* (cm^{-1}) 2478 (B−H). MS (70 eV): *m*/*z* (rel intens) [M$^+$] (40), calcd 718.2200 for $C_{36}H_{49}B_3Ru_2$, found 718.2242.

Table 3. Crystallographic Data and Structure Refinement Information for **9**−**12**

	9	10	11	12
emirical formula	$C_{39}H_{57}B_2Ru_2$	$C_{36}H_{48}B_2Ru_2$	$C_{28}H_{40}B_2Ru_2$	$C_{44}H_{57}B_3Ru_2$
fw	749.61	704.50	600.36	820.47
cryst syst	monoclinic	orthorhombic	triclinic	monoclinic
space group	*P*2(1)/*c*	*Pna*2(1)	*P*$\bar{1}$	*P*2(1)/*c*
a (Å)	16.8511(3)	38.6467(5)	9.0020(2)	11.50010(10)
b (Å)	10.4446(2)	13.3927(2)	9.8968(2)	17.6615(2)
c (Å)	22.1732(4)	12.51440(10)	16.2319(4)	19.6416(3)
α (deg)	90	90	101.611(2)	90
β (deg)	110.362(1)	90	94.952(2)	91.6190(10)
γ (deg)	90	90	103.013(2)	90
V (Å^3)	3658.69(12)	6477.25(14)	1366.95(5)	3987.79(8)
Z	4	8	2	4
D_{calcd} (g/cm^3)	1.361	1.445	1.459	1.367
F(000)	1556	2896	612	1696
μ (mm^{-1})	0.850	0.956	1.118	0.787
cryst size (mm)	0.1 × 0.08 × 0.07	0.14 × 0.06 × 0.06	0.34 × 0.22 × 0.03	0.24 × 0.19 × 0.17
θ range (deg)	1.93−30.51	1.61−32.68	2.17−30.00	1.55−34.55
min and max trans	0.9468, 0.9205	0.9458, 0.8786	0.9694, 0.7024	0.8792, 0.8361
no. of reflns collected	48089	82758	35565	74368
no. of unique reflns (R_{int})	11157 (0.0607)	22263 (0.0285)	7950 (0.0452)	16933 (0.0296)
no. of data/restraints/params	11157/0/419	22263/1/178	7950/0/314	16933/0/468
GOF	1.030	1.048	1.058	1.052
R indices ($I > 2\sigma(I)$)	R1 = 0.0339	R1 = 0.0241	R1 = 0.0335	R1 = 0.0324
	wR2 = 0.0652	wR2 = 0.0528	wR2 = 0.0836	wR2 = 0.0818
R indices (all data)	R1 = 0.0576	R1 = 0.0281	R1 = 0.0437	R1 = 0.0453
	wR2 = 0.0707	wR2 = 0.0536	wR2 = 0.0922	wR2 = 0.0860
largest diff peak and hole (e/Å^3)	0.605, −0.886	0.893, −0.389	2.005, −1.500	2.000, −0.533

Data for 15. $^1H\{^{11}B\}$ (C_6D_6): δ 7.750 (m, 2H, Ph), 7.527 (m, 2H, Ph), 7.342 (m, 2H, Ph), 7.211 (m, 2H, Ph), 7.198 (m, 1H, Ph), 7.136 (m, 1H, Ph), 5.260 (s, br, 1H, B−CH), 4.202 (s, br, 1H, B−Ht), 3.045 (m, 2H, CH_2), 2.500 (s, br, 1H, B−Ht), 2.011 (s, 15H, Cp*), 1.843 (m, 2H, CH_2), 1.585 (s, 15H, Cp*), −10.924 (s, br, 1H, Ru−H(B)−Ru), −11.509 (s, br, 1H, Ru−H(B)−Ru). ^{13}C (C_6D_6): δ 147.41, 141.90, 129.21, 129.10, 128.83, 128.48, 127.00, 126.04 (Ph), 94.48 (Cp*), 89.46 (br, B−C), 86.59 (Cp*), 78.54 (br, B−CH), 36.58 (CH_2), 24.57 (B−CH_2), 12.16, 11.52 (Cp*). ^{11}B (C_6D_6): δ 16.72, 10.30 (1:2). IR (KBr): ν 2495 (B−H). MS (70 eV): *m*/*z* (rel intens) [M^+] (100), calcd 718.2200 for $C_{36}H_{49}B_3Ru_2$, found 718.2189.

Thermolysis of 6 at 90 °C. The solution of **6** (15 mg, 0.02 mmol) in C_6D_6 (0.6 mL) was heated at 90 °C and monitored by ^1H and ^{11}B NMR. **6** is completely converted within 22 h to **14** and **15**.

Conversion of 14 to 15. The solution of **14** (15 mg, 0.02 mmol) in C_6D_6 (0.6 mL) was heated at 84 °C and monitored by ^1H and ^{11}B NMR. **14** is converted into **15** with $t_{1/2}$ = 12 h.

Proton NMR Monitoring the Early Reaction. The reaction of **1** (40 mg, 0.387 mmol) with phenylacetylene (42.6 μL, 1.93 mmol) was monitored in an NMR tube in C_6D_6 (0.6 mL) under argon at ambient temperature. The spectra were recorded on a Bruker AMX 400 spectrometer using a spectral width of 20000 Hz and a relaxation delay of 3 s between pluses. The residual proton signal of the solvent was used as reference (δ 7.16 ppm).

X-ray Crystallography. Crystals suitable for X-ray analysis were obtained by slow evaporation of the hexane solution at ambient temperature. Crystal data were collected on a Bruker Apex system with graphite-monochromated Mo Kα (λ = 0.71073 Å) radiation at 100 K. The structure was solved by direct methods using SHELXS-97 and refined using SHELXL-97 (G. M. Sheldrick, University of Göttingen, Germany). Non-hydrogen atoms were found by successive full-matrix least-squares refinement on F^2 and refined with anisotropic thermal parameters. Hydrogen atom positions were placed at idealized positions except for B−H and Ru−H, which were located from difference Fourier maps. A riding model was used for subsequent refinements of the hydrogen atoms, with fixed thermal parameters [$u_{ij} = 1.2U_{ij}$(eq) for the atom to which they are bonded], again except for B−H and Ru−H, in which case the thermal parameters were allowed to refine independently. Reasonable positions for the missing five hydrogen atoms in **4** and for the missing triply bridging hydrogen atom in **7** could not be located. Their presence is indicated by NMR spectroscopy. The chemical formulas including these hydrogen atoms were used for calculations such as density, molecular weight, and *F*(000). Crystallographic information for the compounds is given in Tables 2 and 3.

Acknowledgment. This work was supported by the National Science Foundation (Grant CHE 9986880).

Supporting Information Available: X-ray crystallographic files (CIF) for compounds **2**, **4**, and **6**−**12**. This material is available free of charge via the Internet at http://pubs.acs.org.

JA042439N